

Nanobiotechnology of protein-based compartments: steps toward nanofactories

1 Andreas Schreiber

Faculty of Biology, Schauenstrasse 1, Freiburg, Germany
Freiburg Institute for Advanced Studies (FRIAS), Albert-Ludwigs-Universität Freiburg, Albertstrasse 19, Freiburg, Germany
Institute for Macromolecular Chemistry University of Freiburg, Freiburg, Germany

2 Stefan M. Schiller Dr.*

Freiburg Institute for Advanced Studies (FRIAS), Albert-Ludwigs-Universität Freiburg, Albertstrasse 19, Freiburg, Germany
Institute for Macromolecular Chemistry, University of Freiburg, Freiburg, Germany



Nanobiotechnology of toroids/donuts, yocrowells, tubes, cages, capsids, compartments and organelles based on protein-building blocks allows for the definition of precise reaction spaces *in vitro* and *in vivo*. Utilizing a synthetic biology approach, the generation of compartment-forming protein 'bio-bricks' points toward new ways to control the assembly of these structures to develop nanofactories *in vivo*. This is envisioned to be an important step allowing for the precise assembly of novel metabolic cascades within nanoreactors in the future. The ability to site-selectively modify proteins by inserting or replacing selected natural and unnatural amino acids at defined positions, provides the necessary tools to control novel functions via 'genetic programming'. The protein-building blocks, already embedded in nature's nanocompartment tool box, will be the focus of this review. The various protein structures forming compartments *in vitro* and *in vivo* will be presented together with their current applications.

1. Introduction

Compartmentalization is a key feature of life essential to orchestrate important cellular processes such as metabolic reactions and the exchange of information. Biological compartmentalization strategies utilize two major components, lipids and proteins. Every cell is enclosed by a lipid membrane separating the interior from the exterior, constituting at least one defined compartment. Although a physical separation between the two environments is usually formed by lipid membranes, protein-based membranes are frequently applied in prokaryotes and eukaryotes as well.¹ Higher cells contain several lipid-enclosed compartments so-called organelles and protein-based structured spaces, for example, the proteasome and vault protein containers. In prokaryotic cells, only a few lipid-enclosed organelles are known, for example within the bacterial phylum of *planctomycetes*² and several protein-based compartments or organelles like the so-called bacterial microcompartments (BCMs). Beside these structures nature uses a large variety of protein-based compartmentalization strategies in the form of virus capsids to package and deliver DNA or RNA.

Mimicking the natural concept of functional compartments has been subject of intensive research for several years.^{3–6} New concepts for the constitution of novel compartments within the cell and pseudo cell-based functional units allow to define a new generation of nanofactories as promising tool for many medical and biotechnological applications.^{4,7} In our vision, protein-based building blocks already utilized by nature, constitute a versatile basis for a structural tool box allowing to create defined spaces *in vivo* and *in vitro*. This provides the ideal platform to develop novel strategies for both bottom-up³ and top-down^{8,9} approaches. While polymer and lipid-based nanoreactors have been exploited by many groups,^{9–12} a growing number of researchers unravel the advantages of protein-based nanocompartments.^{3,13–15} In this review, the authors exclusively focus on protein-based nanocompartments such as toroid cages, capsids and organelles *in vivo* and *in vitro*. Synthetic biology, comprising a multidisciplinary field of chemistry, biology, materials science and pharmacy, aims to rebuild components and architectures of life, such as enzymes, reaction compartments or artificial organelles.¹⁶ In the light of a synthetic

*Corresponding author e-mail address: stefan.schiller@frias.uni-freiburg.de

biology approach, novel possibilities can be used to adapt these compartmentalization strategies.

2. Protein-based 3D structures constituting a defined space

Due to their numerous advantages within the field of nanobiotechnology, the utilization of protein-based 3D structures for *de novo* applications is growing constantly.^{17,18} Major advantages are as follows:

- They can be readily modified by site-specific orthogonal reactions gaining new functionalities.
- They permit a controlled efflux across the protein-based membrane.
- They allow to align and assemble multienzyme cascades in time and space.
- They increase the local concentration of catalysts/enzymes and substrates.
- They help to retain volatile intermediates.
- They enhance the reaction kinetics of metabolic cascades by the above effects.
- They are tunable in size over a broad range.

These features lead to highly controllable reaction environments allowing to utilize protein-based compartments as a system for adjustable reaction platform technologies *in vitro* and *in vivo*.

The structural variability of the different protein subunits constituting nanocompartments, solely based on proteins, allows for the formation of confined spaces in various dimensions (Figure 1). While some nanocompartments are extremely stable, for example, ‘stable protein 1’ (Sp1) which remains stable up to 100°C,¹⁹ others exhibit several constraints regarding their thermal, chemical and proteolytic stability. To overcome these limitations, numerous strategies are being developed, for example, pegylation or genetic engineering, to adapt their properties for technological applications. The use of proteins as building block provides several features unique to protein-based compartments (see above). Besides providing a confined space, the dynamic movement of the protein backbone in combination with the chiral inner and outer surface of the compartments protein surface offers additional elements to control chemical and biochemical reactions. Several methods from synthetic and molecular biology enable to selectively modify the protein backbone with functional groups, for example, introducing surface accessible site chains or unnatural amino acids (UAA).^{20–24} The genetically encoded, site-selective incorporation of UAA-bearing site chains with bioorthogonal reactivity in response to the amber stop codon allows to selectively functionalize proteins or whole protein libraries with chemical libraries *in vitro* and *in vivo*.^{25–29} Hence, the technique of UAA incorporation into proteins has been applied in various fields of biology, for example, the structural analysis of proteins³⁰ *in vivo* labeling³¹ and for protein-protein interaction studies.³² This allows to expand the chemical functionality of *in vivo* systems beyond the reactivities of natural

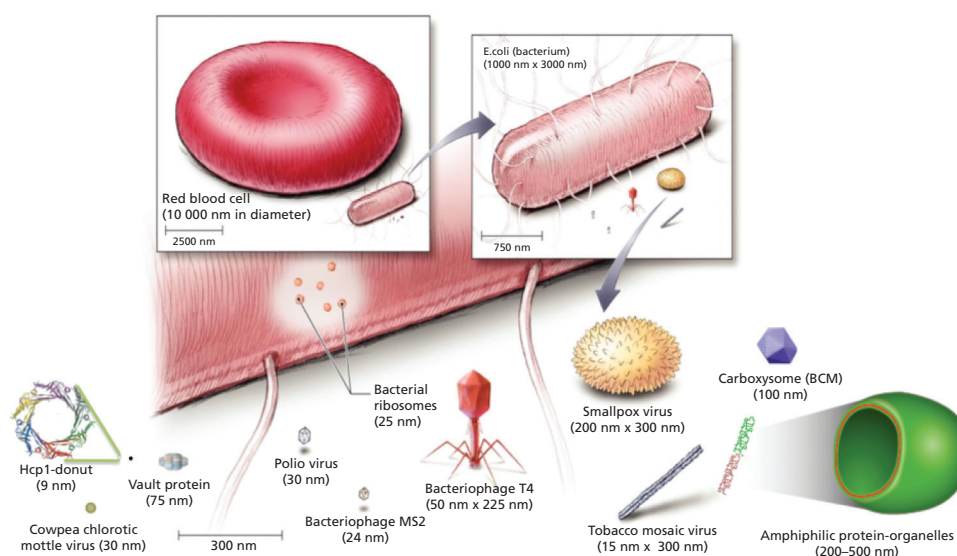


Figure 1. Schematic picture of different protein-based compartments spanning the scale from nano- to micro-scale. Illustrated are toroids/donuts, yoctowells, tubes, cages, capsids, compartments and organelles based on proteins as precise reaction spaces *in vitro* and *in vivo*. Reprinted and modified with the permission from the Pearson Education, Inc., Upper Saddle River, NJ, USA. Copyright© 2007.¹⁸⁰

amino acids and their post-translational modifications creating entirely new structures and modifications. A major emphasis of this review is to provide an overview over the complex tool box of nanostructured protein-enclosed spaces in combination with their functional potential to provide a resource for future reaction engineering within the living cell, for example, assembling novel metabolic cascades (Figure 2), which is still in its infancy stage.

3. Toroid-shaped proteins, donuts, rings and yocotowells

Sp1 (stable protein 1) from *Tremula aspens* is a chaperone-like protein constituting a homododecameric protein ring (Figure 3(c)). The stress and drought responsive protein is boiling, detergent and protease resistant.³³ This structural stability facilitates the use of Sp1 as nanoreactor. Upon assembly of the 12.4 kDa subunits, it forms a ring of 11 nm in diameter with a central pore width of 2–3 nm.^{19,34} Sp1 nanorings have been rendered catalytically active via in situ crystallized palladium particles inside the pore.³⁵ Palladium particle size (2.85 ± 0.5 nm) and position have been controlled by the protein ring as template. The hybrid structure can be utilized to catalyze the reduction of 4-nitrophenol to 4-aminophenol in the presence of NaBH_4 . Hence, not only biomineralization but also new catalytic functions can be implemented by using protein rings as scaffolds. Upon genetical modification, Sp1 could be attached to and released from different surfaces.³⁶ In addition, large periodic 2D arrays and gold nanoparticle protein tubes could be assembled.³⁷ SP1 can thus be envisioned to be used for enzyme cascades or yocotowell-sized reaction arrays. Another ring-shaped protein suitable as nanoreactor is (hemolysin-coregulated protein 1) Hcp1.

Hcp1 is a ‘donut’-shaped homohexameric pore protein from *Pseudomonas aeruginosa*, which was first described by Mougous *et al.*³⁸ It is a central component of the type VI secretion system (T6SSs) and involved in the pathogenicity of several Gram-negative bacteria.^{38–40} Hcp1 has an outer diameter of 9.0 nm, an inner diameter of 4.0 nm and a height of 4.4 nm with a pore volume of about 55 yL ($1 \text{ yL} = 10^{-24} \text{ L}$)³⁸ (Figure 3(a)). The single subunits of Hcp1 can be reversibly assembled and disassembled into toroids, tubes and fibers.^{41,42} Bioconjugation with semiconductor nanoparticles has been achieved using genetically modified Hcp1 as template.⁴³ Beyond the fabrication of protein–nanoparticle composites for imaging and catalysis, protein toroids/rings offer interesting features for the design of new nanofactories. They can be chemically modified by endogenous reactive groups⁴⁴ (e.g. cysteine, lysine, C- and N-terminal positions) already present or genetically introduced.⁴⁵ For example, endogenous lysine residues on the surface of Hcp1 have been used to bind an initiator molecule for atom-transfer radical polymerization (ATRP). From this, hcp1-macroinitiator poly-N-isopropylacrylamide (PNIPAAm) was successfully grafted. Another smart approach for orthogonal chemical modification is the incorporation of UAA by the amber suppression method.^{20,21} This technique allows for the well-defined bioorthogonal insertion of new chemical functionalities into a constrained reaction environment. Utilizing the site-specific attachment of catalytically active molecules to the cavity of the toroid, geometrically constrained reaction chambers can be designed. This approach was used to genetically incorporate a UAA into the inner cage of Hcp1. After the chemical modification of the UAA inside the confined cavity, a *de novo* enzyme (new

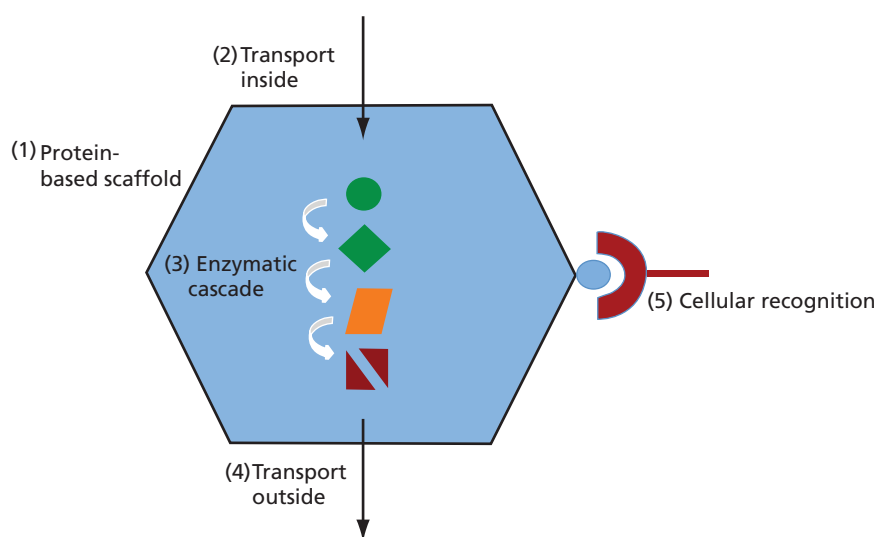


Figure 2. Scheme of a biologically inspired nanofactory (adapted from Ref. 4 featuring) (1) a structural shell or scaffold, (2) transport biomolecules/substrates to and from the environment, (3) encapsulation of a catalytic machinery and (4) cell targeting of the factory.

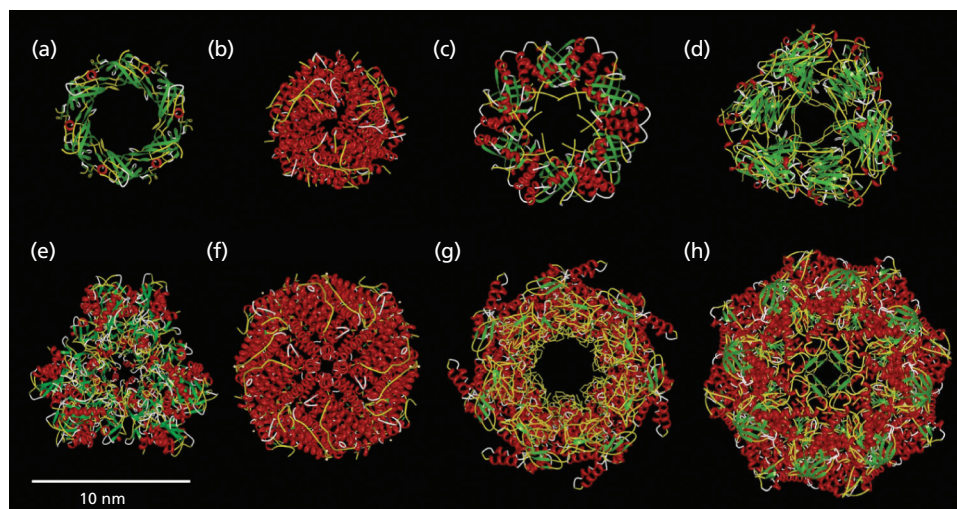


Figure 3. Crystal structures of different-sized protein-based nanocompartments (sizes increase from (a)–(h)): (a) hemolysin-coregulated protein 1 (Hcp1, pdb: 1y12),³⁸ (b) DNA-binding protein from starved cell (Dps, pdb: 1QGH),⁸⁷ (c) stable protein 1 (Sp1, pdb: 1TR0),¹⁹ (d) small heat shock protein (sHSP, pdb: 1SHS),⁸⁸ (e) amino peptidase (PepA, pdb: 3KL9),¹⁰³ (f) apoferritin (pdb: 1DAT),⁷⁹ (g) GroEL (pdb: 1GRL),⁴⁸ (h) THS (pdb: 1A6D).⁵⁵ Secondary structural elements are consistently colored with yellow for random coils, red for α -helices, green for β -strands and white for turns.

functional biohybrid catalyst) could be created. By attaching those functional toroid protein catalysts to a surface, a defined reaction well (yoctowell) with a single substrate entry side can be created (Figure 4).

4. Tubes, barrels and gated protein cylinders

Chaperonins and proteasomes share similar architectural requirements for polypeptide binding and processing. Thermosomes, GroELs and proteasomes exhibit a cylindrical shape and possess a central cavity or channel for protein processing, suitable for nanoreactor applications (see Figure 5).⁴⁶

GroELs are bacterial type I chaperonins consisting of two symmetrical rings with nearly sevenfold rotational symmetry stacked on top of each other.⁴⁷ Every ring contains seven homomers (57 kDa) forming a porous cylinder of 14 subunits with an inner cavity of 4.5 nm in diameter⁴⁸ (Figures 3(g) and 5(a)). The cavity of GroEL assists in refolding of misfolded polypeptide chains. Upon binding of a ring-shaped cofactor (GroES), the chamber is closed by GroES acting as a lid.⁴⁹ After the correct folding, proteins are released from the cavity by an ATP-induced conformational change.^{50,51} Using this mechanism, cadmium sulphide nanoparticles were trapped inside GroEL cavity and subsequently released.⁵² Upon chemical modification

of genetically introduced cysteines, a metal-induced tubular chaperonin assembly could be demonstrated.⁵³ Tubes up to 2.5 μm in length were assembled while disassembly was induced by EDTA addition.

Besides the type I chaperonins, found in the bacterial cytosol and endosymbiotic organelles represented by bacterial GroEL, type II chaperonins can be used as nanoreactors as well.⁵⁴ Chaperonins of type II have a built-in lid and play an important role in cellular protein folding in eukaryotes and archaea.

THS, the archaeal thermosome chaperonin from *Thermoplasma acidophilum* (the eukaryotic homolog to CCT-chaperonin-containing TCP-1) is a spherical, hexadecameric complex consisting of two stacked rings that join at the equatorial plane of the spherical structure⁵⁵ (Figures 3(h) and 5(b)). Each ring is composed of eight alternating α and β subunits of 58 kDa.⁵⁵ THS is about 15.8 nm in diameter and has a built-in lid at its apical domain of each subunit. The closed inner cavity of THS is about 5.4 nm at the upper part and 8.6 nm at the equatorial plane comprising an enclosed volume of approximately 130 nm³,³ able to fully encapsulate proteins up to 50 kDa.^{47,55} The chaperonin-mediated protein folding is dependent on the closure of a built-in lid⁵⁶ and is triggered by ATP hydrolysis.^{57,58} In the open nucleotide (ATP) unbound state, THS was used as reaction compartment by Bruns *et al.* for the ATRP of PNIPAAM. Due to the size limit of the cavity,

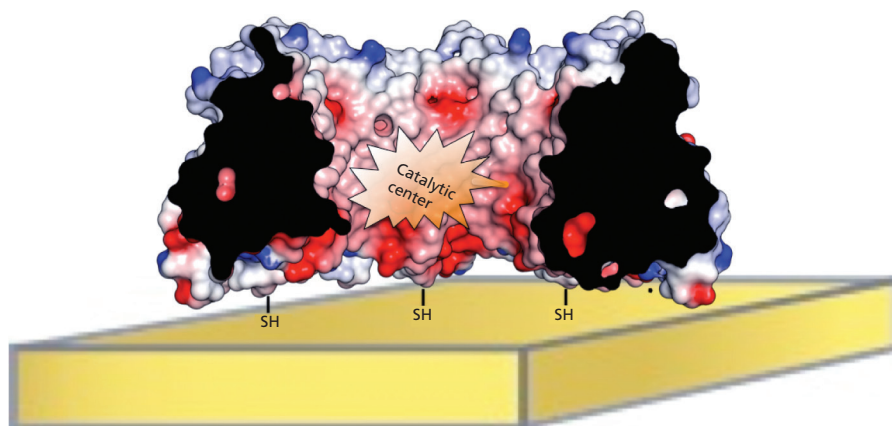


Figure 4. Side view of the Hcp1 yocrowell ($1 \text{ yL} = 10^{-24} \text{ L}$), which is site-selectively modified via the incorporation of unnatural amino acids conjugated with a catalytic reaction center. By attaching this nanocompartment via thiol chemistry to the surface (e.g. gold), a single substrate entry site and constrained well-like reaction compartment is created.

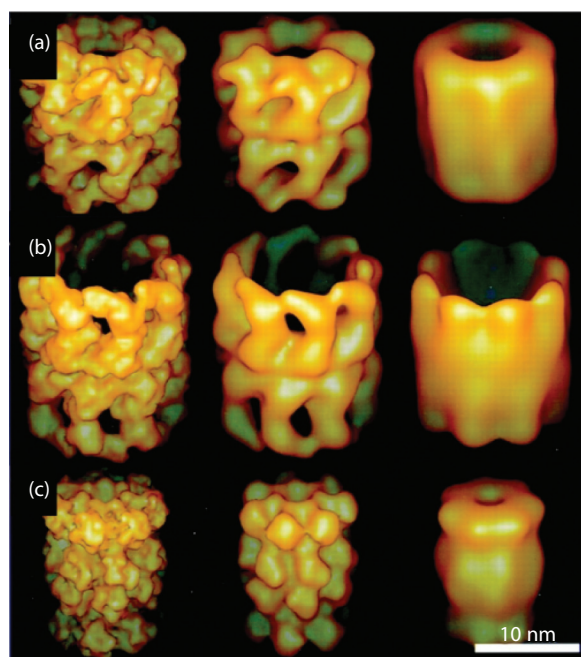


Figure 5. Surface representations and structural similarity of the crystal structures of (a) GroEL from *Escherichia coli* ($d = 15 \text{ nm}$) with a sevenfold rotational symmetry, (b) the thermosome from *Thermoplasma acidophilum* ($d = 16 \text{ nm}$) with an eightfold rotational symmetry and (c) the 20S proteasome of *Saccharomyces cerevisiae* ($d = 12 \text{ nm}$) with a sevenfold rotational symmetry. The particles were filtered to 2-, 4- and 8-nm resolution (from left to right). Reprinted with the permission from the National Academy of Science Copyright© 2000.¹⁸¹

the ATRP yielded a size-restricted polymer with a polydispersity index as low as 1.11.⁵⁴ Moreover, THS was used as fluorescence resonance energy transfer (FRET)-based mechanical nanosensor for the detection of polymer damage.⁵⁹ A FRET pair was linked into the THS cavity (THS-eCFP-eYFP) and subsequently attached to the target polymer. Polymer stretching associated with chaperonin deformation could be detected by the altered FRET signal intensity.⁵⁹

20S and 26S proteasomes are responsible for the degradation of most cellular proteins via an ATP-dependent proteolytic pathway. The 700 kDa 20S proteasome, also part of the 26S proteasome contains multiple peptidase activities that function through a proteolytic mechanism involving threonine in their active site. The cylinder-shaped 20S proteasome consists of four stacked heptameric rings with two outer α -subunit rings framing two central head-to-head-oriented rings containing catalytic β subunits (Figure 5(c)). Structural analysis showed that the α and β subunits from *Thermoplasma acidophilum* have a common fold, characterized by a sandwich of two β sheets each consisting of five strands, surrounded by two α helices on each side. The complete cylinder has a diameter of roughly 12 nm and a length of 17 nm.⁶⁰ X-ray analysis⁶¹ has confirmed that the *T. acidophilum* 20S particle is a barrel-shaped cylinder (14.8 nm by 11.3 nm in diameter) with a penetrating central channel and three large internal chambers. Its entrance through the outer α rings is only 1.3 nm in diameter, which is only slightly larger than the diameter of an α helix, insufficient to allow the entry of folded proteins. Accordingly, only fully unfolded and reduced proteins can be digested by this particle, as shown for α -lactalbumin which is only degraded in its linearized form.⁶² *E. coli* is lacking a proteasome and therefore a well-suited

host to produce heterologous proteasomes or their subunits in large quantities without interfering with endogenous functions.⁶³ Since peptidases are known to catalyze the peptide bond formation with several substrates,^{64–66} engineering the proteasomes may allow to gain access to novel synthetic features for this interesting nanoarchitecture. Serine peptidases can also exhibit peptide bond formation via the aminolysis of esters, thioesters and amides in accordance with their hydrolytic activity.^{64,67} Exchanging the catalytic Ser for Cys allows to engineer the serine endopeptidase into a ‘transpeptidase’ for peptide bond formation.^{68,69} Thus, it can be envisioned that the catalytic functionality of the proteasome can be altered in the future.

The 26S proteasome is a 2 MDa complex degrading ubiquitinated proteins in eukaryotes. In addition to the 20S proteasome, it also contains a 19S regulatory complex composed of several ATPases and further components necessary for substrate binding. The 26S proteasome has an important ATP-dependent proteolytic function, but is also involved in many nonproteolytic cellular activities often mediated by subunits in its 19S regulatory complex. It consists of more than 30 different protein subunits with a barrel-shaped 20S protease core particle formed by the axial stacking of four heptameric rings composed of two identical inner β rings, each formed by seven different β subunits $\beta 1$ – $\beta 7$ and two identical outer α rings each formed by seven different α subunits, $\alpha 1$ – $\alpha 7$. Until now, it was not possible to crystallize the entire 26S proteasome for structure determination by X-ray crystallography.⁷⁰

5. Protein cages

Protein nanocages provide defined sizes at the nanometer scale, precise sterical characteristics and tunable charge distributions resulting in a distinct interaction pattern with potential reaction partners. They are used as templates for defined nanoparticles (NPs) synthesis,^{71–73} nanobiohybrid assembly^{35,43} and if NPs are deposited inside the protein cage, they can enhance endogenous enzymatic activity^{74,75} or exert new catalytic reactions.⁷⁶ In contrast to virus capsids, their known variety in size and shape is significantly smaller (Figure 3).

Ferritin, belongs to a family of iron storage proteins found in cells and in extracellular matrices⁷⁷ throughout the plant, animal and microbial kingdoms.⁷⁸ The first well-characterized ferritin, isolated from horse spleen, is a 450 kDa protein and assembles from 24 subunits into a spherical cage of 12 nm in diameter and an inner cavity of 8 nm⁷⁹ (Figure 3(f)). The inner cavity of ferritin permits the storage of up to 4500 iron atoms,⁸⁰ which serve as a reservoir for metabolic use. By removing the iron cluster from the cavity, the protein coat remains, called apoferritin. Eight hydrophilic pores (4 nm in width) facilitate the transfer of iron atoms and other molecules through the protein shell. Ferritins are among the first well-studied nanocages. Because of its metal binding capacity, horse

spleen apoferritin has been used as a scaffold for the synthesis of different inorganic nanoparticles within the inner space,^{6,81,82} which are described in detail elsewhere.³ The first biocatalytic reaction inside the apoferritin was conducted by the group of Watanabe and coworkers.⁸³ They reduced Pd^{2+} ions in situ inside the central cavity to palladium clusters which were shown to size-selectively hydrogenate olefins. Because of their eight negatively charged pores, substrate diffusion to the center is dependent on substrate charge and size, which as consequence determined the turn over rates. Moreover, the Watanabe group immobilized Rh^{2+} complexes inside the apoferritin cage to catalyze the polymerization of phenylacetylene in aqueous media.⁷⁷ The resulting polymers from the protein nanoreactor showed a restricted molecular weight and a narrower molecular weight distribution than those polymerized without the cage. By combining protein cages as soft scaffolds and Pt-NP as active reaction site, Douglas, Young and colleagues could build functional artificial hydrogenases. Mimicking the function of hydrogenases, they used Ferritin,⁸⁴ Dps (DNA-binding protein from starved cells) from the Gram-positive bacterium *Listeria innocua*⁸⁵ and small heat shock protein (sHsp) from *Methanococcus jannaschii*⁸⁶ as cages. Dps are part of the subfamily of ferritins and prevent oxidative damage of DNA in starving cells by accumulating iron atoms within their central cavity to produce an iron oxide core binding the DNA.⁸⁷ It is composed of 12 identical 18 kDa subunits forming a hollow protein cage of tetrahedral symmetry (Figure 3(b)). The outside (9 nm in diameter) and the inner cavity (5 nm in diameter) are linked through pores with 0.8 nm in diameter, where molecules can pass through.⁸⁷ Ferritin-Pt and Dps-Pt composites were first used for efficient proton reduction, which was driven by light and coupled to $\text{EDTA-Ru}(\text{bpy})_3^{2+}$ and methyl-viologen as electron-transfer mediators. Enhancement of the endogenous catalytic activity of ferritins by NP deposition could also be shown. The activity of ferroxidase–apoferritin was increased multiple folds by silver, gold and platinum nanoparticle deposition inside the ferritin protein nanocage.^{74,75}

Hsps are expressed in response to cellular stress to help in the correct folding of proteins. Archaeal sHsp from *Methanococcus jannaschii* (Mj) assembles from 24 subunits of 16.5 kDa into a 12 nm cage at the outside and 6.5 nm at the inside⁸⁸ (Figure 3(d)). Eight pores of 3 nm at the threefold and 1.7 nm pores at the fourfold axis allow for molecular trafficking. A high cage stability of sHsp up to 70°C and a broad pH range tolerance from 5 to 11⁸⁹ permits its use as nanoreactor. MjsHsp was used for the polymerization of branched polymers inside the cavity, which increased its stability up to 120°C.⁹⁰ In addition, platinum nanoparticles (Pt-NP) incorporated into the cavity of MjsHsp were used to catalyze hydrogen production.^{84,85} When compared under the same conditions, ferritin (see above) excelled the hydrogen production of MjsHsp. Modifications with organic molecules outside and inside of MjsHsp led to new functionalities.⁹¹ Douglas and coworkers demonstrated cell targeting using MjsHsp.⁹² By fusing an RGD-aminoacid sequence for cell recognition to the

outside of MjsHsp and an imaging agent at the inside, sHsp was used to image melanoma and lymphocyte cells. This example demonstrates the possibility to shuttle nanocontainers to specific targets and reaction sites of interest (Figure 2).

Fungal fatty acid synthase (FAS), pyruvate dehydrogenase complexes (PDH) and lumazine synthase are multienzyme compartments in which the enzymes themselves form the wall of the compartment.

Fungal FAS from *Thermomyces lanuginosus* consists of a 2.6-megadalton $\alpha_6\beta_6$ heterododecameric complex.⁹³ The size of the complex is relatively large compared with mammalian FAS, a 540-kD α_2 homodimer.^{94,95} Six catalytic domains formed by the α - and β -polypeptide chains form the FAS together with numerous expansion segments responsible for extensive intersubunit connections. The barrel-like cage has an outer height of 27 nm and a diameter of 25 nm. Despite its potential as nanoreactor, no applications have been reported so far.

PDH complexes contain a pyruvate decarboxylase (E1), a dihydrolipoyl acetyltransferase (E2), a dihydrolipoyl dehydrogenase (E3) and in the case of mammalian enzymes kinases, phosphatases and an E3-binding protein. Sixty copies of the E2 protein interact via their catalytic domains forming an icosahedral structure⁹⁶ to which other subunits can bind complementing this structure. The E2 subunit-formed shell has a diameter of 24 nm with 12 pores of 5 nm in diameter. The complex is found in the mitochondria of eukaryotes and Gram-positive bacteria⁹⁶ and is stable at relatively high temperatures of roughly 80°C.^{97,98} Reported applications include the use as molecular carrier⁹⁸ and the display of epitopes from circumsporozoite proteins of *Plasmodium falciparum* and *Plasmodium berghei* and enhanced green fluorescent protein (GFP).⁹⁹ In contrast to other protein-based compartments, PDH itself forms the walls of the enzyme complex allowing substrates to enter but excluding other macromolecules.

Lumazine synthase consists of 60 subunits forming a 1 MDa bacterial enzyme complex involved in the synthesis of lumazine, a precursor of riboflavin. It exhibits an icosahedral symmetry with an outer diameter of 14.7 nm and an inner diameter of 7.8 nm with a negative charge at the inside of the cage due to the presence of glutamate residues.⁹⁹ The cage is highly stable at pH 7 in the presence of phosphate buffer or its substrates, forming larger particles of 30 nm when substrates are absent.¹⁰⁰ Similar to PDH, the enzyme itself forms the wall of the protein cage. Lumazine cages have been utilized for biomineralization studies of iron ions yielding cages with 20-nm inner diameter and 30-nm external diameter at pH 6.5 and no ligand-efforting iron nanoparticles of 10–15 nm in size.¹⁰¹ An interesting encapsulation approach using lumazine was achieved by mutating four residues per subunit to glutamate (cages contain 60 or 180 subunits) pointing toward the lumen of the cage creating 240 or 720 additional negative charges within the interior.

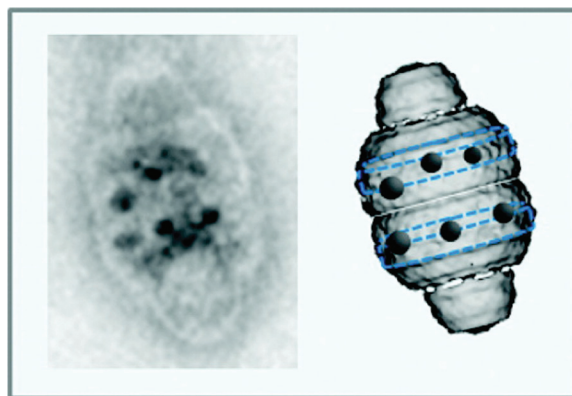


Figure 6. Negative-stain TEM image (left) and corresponding cartoon of the vault protein enclosing gold nanoparticles. Reprinted with the permission from the American Chemical Society Copyright© 2009. TEM, transmission electron microscopy.¹⁰⁷

This negatively charged lumazine was expressed in *E. coli* and is stable at temperatures up to 95°C. Due to its negatively charged interior, it could effectively been used to encapsulate positively tagged (R_{10} -tag) proteins, for example, GFP.¹⁰²

Aminopeptidase (PepA) from *Streptococcus pneumonia* is a tetrahedral dodecameric bacterial aminopeptidase-forming cages with 12 nm in diameter at the outside and 6 nm at the inside.^{76,103} From the faces and edges of the tetrahedron, eight channels (1–3 nm in width) span to its center cavity to allow substrate transport. The metallopeptidase, which hydrolyses oligopeptides in bacteria into free amino acids was used for templated Pt-NP deposition. Most catalytically active protein cage-metal composites exert their activity through their active metal site. By combining the catalytic properties of Pt and aminopeptidase as protein cage, a multifunctional biohybrid catalyst has been constructed.⁷⁶ Subsequently, the aminopeptidase-Pt biohybrid could be shown to catalyze the hydrogenation of p-nitrophenol as a substrate and at the same time hydrolyses glutamic acid-p-nitroanilide. As common for catalysts, both peptidase and hydrogenation activities were indirectly proportional to the Pt-NP size.⁷⁶

Vaults are large cytoplasmic ribonucleoprotein particles of eukaryotic cells¹⁰⁴ of roughly 13 MDa. They are composed of 96 copies of the major vault protein (MVP), telomerase-associated protein 1 (TEP1), vault poly(ADP ribose) polymerase and untranslated vault RNA. Their maximal dimensions are 42 × 75 nm and they possess eight small holes with a diameter of 2 nm (Figure 6). The possibility to incorporate a large number of molecules might play a role in multidrug resistance.¹⁰⁵ Analyzing the vault structure indicates that vaults can enclose complexes up to 330 Å in diameter. Compared with the maximum dimension of the ribosome (~278 Å),¹⁰⁶ it could easily fit into the vault. In analogy to this example, the volume of the vault can be calculated

to $5 \times 10^7 \text{ \AA}^3$ which is more than 500 times the volume of the cavity in GroEL and GroES.¹⁰⁵ Recombinant MVP expressed in insect cells is sufficient to form vault nanocages. Several applications have been already tested including the application of vaults as nanoshuttle for gold and proteins probes¹⁰⁷ and the engineering of vault capsules with enzymatic and fluorescent properties.¹⁰⁸

6. Virus capsids and rods

Virus-derived structures and virus-like particles (VLP) could be systematically added to the protein cages paragraph. Due to their huge impact and significantly larger variety in size and space, they are listed separately within this chapter. Even though filamentous viron assemblies usually do not provide a protein-enclosed free space due to their assembly around negatively charged macromolecules such as DNA and RNA, they are important protein structures used to immobilize nanoparticles and enzymes. Viruses are protein-based cages of 15–400 nm in size,¹⁰⁹ whereas some references state 18–500 nm¹¹⁰ enclosing genetic information within their coat. In some cases, virions can undergo reversible structural changes, for example, changing between open and closed pores allowing to provide a switchable access to the capsid interior, for example found for chlorotic mottle viruses. Virus capsids present the group of protein-cage structures with the largest known number of applications. Viruses have been used as templates for the synthesis of various hybrid materials,^{111,112} as platform technologies for diagnostic imaging¹¹³ and novel metallic, magnetic and semiconducting nanomaterials.^{114,115} Their applications span a wide range from nanostructured materials, nanocircuits, nanoelectronics, light harvesting systems, drug delivery, biomedical applications, biomineralization, to the encapsulation of small and large molecules, nano-organization, biosensing and catalysis.¹¹⁶

6.1 Spherical virus geometries

CCMV (cowpea chlorotic mottle virus) is a very well-studied icosahedral plant virus, named after the appearance of yellow spots on affected plants (e.g. cowpeas) with an outer diameter of 28 nm. The protein shell, which is composed of 180 identical 20 kDa capsid proteins defines an inner cavity of 18 nm encapsulating single-stranded RNA.^{117,118} Each subunit contains nine positively charged basic amino acids (lysine and arginine) which can be exchanged against acidic residues without disrupting the assembly properties of the capsid shell.¹¹⁹ Young *et al.* genetically designed the negatively charged cage interior for confined iron oxide particle formation.¹¹⁹ Using the wild-type capsids for biomineralization, TiO_2 ,¹²⁰ paratungstate, decavanadate¹²¹ and prussian blue nanoparticles¹²² could be deposited inside CCMV capsids as well. Besides the entrapment of MRI contrast agents,¹²³ drugs¹²⁴ and anionic polymers,¹²¹ single enzymes¹³ could be encapsulated forming a catalytic active nanofactory. CCMV can assemble in the absence of RNA into empty viron particles^{119,125} and reversibly disassemble at pH

7.5, which is very suitable for the application as nanoreactor. Moreover, pH-dependent reversible capsid expansion where the protein cage swells by 10% has been described.¹²⁶ By lowering the pH (pH 5), single horseradish peroxidase (HRP) enzymes could be entrapped inside the CCMV capsid. The encapsulated HRP catalyzes the reaction of a nonfluorescent substrate to a highly fluorescent product. By raising the pH > 6.5 in the absence of metal ions, the capsid swells and 60 pores of 2 nm in diameter are formed.¹¹⁷ Increasing the pH was correlated with a higher product diffusion monitored by fluorescence correlation spectroscopy. Additionally, Minten *et al.* could show multiple protein encapsulation into CCMV capsids.¹²⁷ By using genetically modified heterodimeric coiled coil protein ends at the target protein (EGFP) and at the CCMV; EGFPs can assemble together with the CCMV capsid shell. In this way, up to 15 EGFP proteins per capsid were encapsulated in a controlled and efficient way.¹²⁷ Using the same strategy, Minten *et al.* could entrap multiple functional enzymes of PalB (pseudozymantartica lipase B).¹²⁷ PalB inside the nanocage compared with free PalB did convert the substrate more efficiently. While increasing amounts of PalB inside CCMV decreased the conversion rate owing the fact that substrate is the limiting factor rather than enzyme concentration. The encapsulation of different active enzymes might pave the way toward enzymatic cascade reactions in confined protein cages as shown in Figure 2.

Cowpea mosaic virus (CPMV) is a comovirus and belongs to a group of plant viruses of the picornavirus superfamily with an icosahedral envelope. CPMV was crystallized in the cubic space group I23, $a = 317 \text{ \AA}$ and the hexagonal space group P6122, $a = 451 \text{ \AA}$, $c = 1038 \text{ \AA}$. The capsid with a size of roughly 300 Å is similar to the picornavirus capsid displaying a pseudo $T = 3$ ($P = 3$) surface lattice. The CPMV capsid comprises large (200 Å) solvent channels in the lattice allowing exchange of CPMV cognate Fab fragments.¹²⁸ The capsid has been used for the development of virus-based nanoparticles (VNPs) as platform technology for diagnostic imaging,¹¹³ the modification of the capsid with small organic molecules inside or outside, verified via the attachment of antibodies,¹²⁹ and as icosahedral template for polyvalent carbohydrate display platforms.¹³⁰

The bacteriophage MS2 consists of an icosahedral capsid comprised of 180 identical protein units. The capsid has a diameter of 27 nm comprising 32 pores with 1.8 nm in diameter. Its structure is similar to that of CPMV. It has been utilized as template for Diels–Alder reactions,¹³¹ MRI agents¹³² and osmolyte-mediated encapsulation of proteins inside MS2 viral capsids.¹³³

Bacteriophage Q β forms icosahedral VLPs embedding 180 copies of the 14.3-kDa coat protein (CP) to form a RNA-directed encapsidation system of target enzymes. The group of M. G. Finn reported the packaging of the 25 kDa N-terminal aspartate dipeptidase, peptidase E (PepE), the 62 kDa firefly luciferase

(Luc) and a thermostable mutant of Luc (tsLuc) inside VLPs. The system is composed of a cargo enzyme N-terminally tagged with a Rev-peptide (arginine-rich peptide), the coat protein and a two binding domain containing CP-RNA (consisting of the CP-RNA, a Rev-binding aptamer and a Q β genome packaging hairpin (hp) binding the interior of the CP). The Rev-tagged cargo enzyme binds the arginine-rich peptide (Rev) binding aptamer, part of the CP-RNA, which binds the CP via a Q β genome packaging hairpin thus allowing to genetically encode all components required for the formation of enzyme-loaded viral particles (VP).¹³⁴

The Poxvirus D13 Virus capsids are unusual since they have a brick shape and lack symmetry. In the case of vaccinia virus, trimers of the 63-kDa D13 polypeptides form the building blocks of a capsid lattice.¹³⁵ D13 is homologous to capsid proteins of icosahedral DNA viruses, it is able to form sheets of some 100-nm tubes and 300–400-nm spheres. The structural variability, especially ordered sheets, will allow for applications different from standard capsid structures.¹³⁶

Brome mosaic virus has a triangulation number of $T = 3$, is composed of 180 proteins and a RNA-controlled polymorphism is known to occur. 180- and 120-subunit virions were induced to assemble *in vivo* with engineered mRNA. It is capable to form empty capsids with sizes varying from 20 to 29 nm and shows a swelling transition. It is most stable at low to moderate ionic strength at a pH lower than 5.0 and undergoes a structural transition upon a pH change from 5 to 7 (as found in other virus capsids, e.g. CCMV). Magnesium ions stabilize the 28-nm-sized capsid around neutral pH where reversible capsid expansion without dissociation occurs. Carboxylate-functionalized gold nanoparticles with a size of 16–17 nm were encapsulated with 95% yield into the inner space of the cage (17–18 nm).¹³⁷

Bacteriophage P22 VLP capsid derived from *Salmonella typhimurium* is composed of 420 copies of a 46.6-kDa coat protein (CP) that assembles into a $T = 7$ icosahedral capsid with the aid of approximately 100–330 copies of a 33.6-kDa scaffolding protein (SP). Heterologous expression of P22 CP together with SP leads to self-assembly of the compact procapsid (PC) structure with an external diameter of 58 nm. An interesting characteristic of the P22 VLP capsid is the ability to modulate the overall volume and porosity. This feature allows to adopt its properties and to fine tune them for biocatalytic applications. Gently heating the capsid for 10 min at 65°C leads to an expansion of the capsid to irreversibly form the 64 nm P22 structure referred to as expanded form. This structural change leads to near doubling of the effective volume from 58 000 nm³ in PC to 113 000 nm³ in the expanded form.¹³⁸ P22 bacteriophage capsid has been used to encapsulate the thermostable tetrameric CelB glycosidase creating catalytically active nanoreactors. These nanoreactors maintain their ability to undergo morphological transitions by modifying the VLPs internal volume and shell porosity.¹³⁹ Utilizing alcohol dehydrogenase D (encapsulating AdhD), the Douglas group was able to achieve high

loading ratios of the enzyme into P22 capsids affecting its kinetic parameters.¹³⁸

SV40 is composed of 72 pentamers of the VP1 major capsid, the minor capsid protein VP2 and its aminoterminal truncated form VP3, whereas the latter one has unknown physiological functions. Under physiological salt and pH, VP1 is dissociated while at pH 5.0, it assembles into tubular structures of 40–45 nm in diameter.¹⁴⁰ A combination with a stoichiometric amount of VP2 allows the assembly of VP1 pentamers into spherical structures at a pH between 4.0 and 7.0.¹⁴¹ SV40 has been exploited as delivery vehicle for biomolecules with a focus on DNA delivery for gene therapy.^{142,143} Catalytic functions of SV40 have been investigated utilizing different model proteins. The encapsulation of proteins was demonstrated utilizing a VP2/3 fusion protein with EGFP as a model protein. It was found that fusion to the C-terminus of VP2/3 is preferable and that the C-terminal VP1-interaction domain of VP2/3 is sufficient for incorporation into VLPs. Using this system, yeast cytosine deaminase, a prodrug-modifying enzyme can be encapsulated in VP1-VLPs by fusion to VP2/3 and successfully delivered to cells.¹⁴⁴

6.2 Elongated and rod-like virus geometries

Rod-like viruses architectures are special since their assembly relies on negatively charged cores enclosed by the capsid proteins.

Potato virus X forms flexible rod-like structures based on 1270 identical capsid proteins with a molecular weight of 25 kDa per capsid forming a rod of 500 nm length and 13 nm in diameter.¹⁴⁵ It has been used to present peptides of biopharmaceutical interest¹⁴⁶ and for bioconjugation of potential therapeutic molecules.¹⁴⁷

The M13 bacteriophage infects *E. coli* cells causing chronic infections allowing infected cells to continue to grow and divide, although at a lower rate than normal. The phage particle adopts a cylindrical shape with a diameter of 6.5 nm and 900 nm in length. The flexible filament contains a circular, single-stranded viral DNA genome composed of 6407 nucleotides, protected by a long cylindrical protein coat consisting of approximately 2700 copies of the major coat protein gp8 capped by the minor coat proteins (3–5 copies each) gp3 and gp6, or gp7 and gp9 at both ends. The viral DNA is surrounded by the major coat protein forming a tube in an overlapping helical array. The proteins of the coat are oriented in a way that the N-terminus is located at the outside of the coat and the C-terminus interacts with the DNA at the inside of the coat. The hydrophobic domain of the major coat protein is located in the central part of the protein and interlocks the protein with its neighboring coat proteins in the VP. The amino acid sequence consists of domains where the amino acid from 1 to 6 are acidic, 7 to 20 are amphiphatic, 21 to 39 are hydrophobic and 40 to 50 are basic. The strong C-terminal interfacial anchor leads to an effective embedding of the protein in the bacterial membrane,

which together with a simple tilt mechanism and a subtle structural adjustment of the extreme end of its N-terminus provides favorable thermodynamical association of the protein in the lipid bilayer.¹⁴⁸ The M13 bacteriophage has an enormous amount of nanobiotechnological applications. It has been used successfully to immobilize biocatalysts, for example, Candida Antarctica lipase B (CALB) by the groups of Nolte and van Hest¹⁴⁹ and nanoscale ordering of metal nanoparticles or quantum dots.^{113,116} Additional applications include the design of anode materials for lithium ion batteries¹⁵⁰ and the assembly of multilayered polymer surfaces.¹⁵¹

The tobacco mosaic virus (TMV) forms a tube-like structure with a length of 300 nm determined by the length of the underlying 6395 nucleotides of the RNA scaffold. The nucleoprotein tube has an outer diameter of 18 nm and a hollow channel with a diameter of 4 nm.¹⁵² The highly defined nanostructures formed are able to resist temperatures up to 80°C. Without destruction of its integral shape, TMV can be handled in a pH range between 2.8 and 8.0 for a fairly long time (min to h) and it can be dried building a crystal-like structure without destruction of the single virions.¹⁵³ TMV nanostructures have been widely used for many applications. For example, the use of RNA-directed self-assembly of TMV-derived coat protein on a surface immobilized RNA scaffold allows to grow nucleoprotein nanotubes within defined surface structures.¹⁵² The virus-templated synthesis of ZnO nanostructures and the formation of field-effect transistors¹⁵⁴ has been realized as well as the self-assembly of metal-virus nanodumb bells based on Au¹⁵⁵ and the electroless synthesis of 3-nm-wide alloy nanowires,¹⁵⁶ to mention only a few applications.

7. BMCs and nanocompartments

Subcellular compartmentalization was thought to be restricted to eukaryotes for a long time. Isolated in the 1970s, organelle-like structures were found in prokaryotes as well.^{157,158} Many bacteria contain nano- and microcompartments constituted by self-assembling protein-only shells. These structures show a structural diversity and form, by combinations of a small number of repeat elements, ‘nano- or microcompartments’. They range from 60 copies of one protein element self-assembling into 24-nm sized so-called encapsulins also referred to as linocin-like proteins¹⁵⁹ to structures formed from 10 000 or 20 000 copies of a few protein species self-assembling into microcompartments (BMCs) with 100–150 nm in diameter.¹⁶⁰ These BMC organelles are composed entirely of proteins, resembling virus capsids¹⁶¹ and serve as organelles promoting specific metabolic processes by sequestering and protecting enzymes in a defined microenvironment.¹⁶² In contrast to higher cells, their known functional repertoire is restricted to a few pathways.¹⁶³

7.1 Bacterial nanocompartments

Encapsulin crystal structure analysis of particles from *Thermotoga maritima* revealed that 60 copies of the monomer assemble into an icosahedral shell with a diameter of 24 nm. The 31-kDa monomer

is structurally similar to viral capsid proteins. The inner surface of the compartment is lined with conserved binding sites for short polypeptide tags present as C-terminal extensions of enzymes involved in oxidative-stress response. A BLAST search of *T. maritima* encapsulin revealed 49 homologous proteins. Almost all of these proteins are part of an operon that codes for two proteins, where the gene for encapsulin lies downstream. Twenty-eight cases provide a specific type of peroxidase (referred to as dyedecolorizing peroxidase, DyP19) *B. thetaiotaomicron* and in 17 cases, the preceding protein is related to ferritin (ferritin-like protein) from *N. europaea*.

7.2 Bacterial microcompartments

BMCs exhibit a protein shell structure/polyhedron-shaped bodies ranging in size from 80 to 200 nm.¹⁶⁴ The systems which have been in the focus of the current research include the carboxysome, the 1,2-propanediol utilizing (Pdu) BMC and the ethanolamine-utilizing (Eut) BMCs.^{161,163–165} Each microcompartment consists of two or a few distinct enzymes allowing to support a defined number of catalytic reactions. Fully assembled BMCs were purified after recombinant expression but no successful *in vitro* assembly of BMCs is known yet. Pores formed at the corners of oligomerized shell proteins have a typical diameter between 0.4 and 1.6 nm.^{166,167}

Carboxysomes serve as metabolic modules for carbon dioxide fixation, a nice scheme can be found by Kinney *et al.*,¹⁶⁸ also highlighting the structural assembly and pore structure of carboxysomes. Carboxysomes comprise a semipermeable proteinaceous shell mainly comprised of small proteins (roughly 100 amino acids)¹⁶⁸ that encapsulates most, if not all, cellular ribulose-1,5-bisphosphate (RuBP) carboxylase/oxygenase (RuBisCO). RuBisCO enzyme catalyzes the first step in the Calvin–Benson cycle by combining carbon dioxide and RuBP to form two molecules of 3-phosphoglycerate (3PGA) and carbonic anhydrase which converts bicarbonate to carbon dioxide.^{168,169} The α -carboxysome (e.g. *Halothiobacillus neapolitanus*) is formed from CsoS1A, B, C, D and CsoS4A/B encapsulating the enzyme IA RuBisCO while β -Carboxysomes (e.g. *Synechocystis PCC6803*) utilize the BMC proteins CcmK1, 2, 4 and CcmL encapsulating the enzyme IB RuBisCO.^{168,170} Due to the overwhelming importance of cyanobacteria facilitating a large fraction of photosynthesis-based energy conversion and biomass production on the planet, the carboxysome plays a significant role in this context. In the case of carboxysomes, the pore regions are lined by positively charged amino acids and are believed to facilitate the uptake of negatively charged substrates such as bicarbonate and ribulose bisphosphate into and the product 3PGA out of the BMC. The conservation of volatile metabolites such as carbon dioxide and acetaldehyde may be a role for carboxysome-like organelles in *Salmonella enterica*.¹⁷¹

The Pdu compartment from *Salmonella enterica* harbors the coenzyme B12-dependent catabolism of 1,2-propanediol.

1,2-propanediol is produced by the degradation of plant cell wall sugars fucose and rhamnose under anaerobic conditions, serving as energy and carbon source used by bacteria growing in aquatic sediments and a number of enteric bacteria. The catabolism of 1,2-propanediol requires a complex coenzyme-B12-dependent pathway ultimately providing the cell with propionyl-CoA and ATP.^{166,172} The BMC protein typically found is about 90 amino acids in length and adopts an α/β fold.¹⁷³ BMC proteins self-assemble to form cyclic, disc-shaped hexamers constituting the basic building blocks of the compartment. Each hexamer typically provides a narrow pore through the middle, along the sixfold axis of symmetry. PduA, the major shell component constitutes the BMC together with the pore-forming protein PduT and the PduU protein as minor shell component.¹⁷³ BMC proteins can form true 2D layers at the air–water interface of a liquid droplet, with packing parameters seen in 3D crystals as well. The shells formed by these extended arrays build a tightly packed molecular layer perforated by narrow protein pores spaced less than 70 Å apart allowing access to the shells interior.¹⁷³ Pdu-cages can be used to selectively encapsulate proteins utilizing the fusion of the 18 amino acid N-terminal sequence of PduP to glutathione S-transferase, maltose-binding protein or GFP.¹⁷²

Ethanolamine utilization (Eut) based on BMCs, is present in several bacteria, including *Salmonella enterica* and *Escherichia coli*. The Eut microcompartment shares a number of homologous enzymes with a Pdu microcompartment; both metabolic pathways proceed via aldehyde intermediates, propionaldehyde in the case of Pdu and acetaldehyde in the case of Eut. The cellular function of the Eut microcompartment is assumed to metabolize ethanolamine without the release of acetaldehyde into the cytosol thus mitigating the potentially toxic effects of excess aldehyde in the bacterial cytosol preventing the volatile acetaldehyde from diffusing across the cell membrane leading to a loss of carbon for the cell.¹⁷⁴ EutS, EutL, EutK and EutM are thought to be the major shell constituents of a functionally complex Eut microcompartment,¹⁷⁴ interestingly, a minimal Eut BMC that was morphologically similar to the wild-type Eut BMCs can be formed by expression of EutS alone in *E. coli* (Figure 7).^{169,174} The utilization and adaption of BMCs as customizable nanobioreactors requires the targeting of heterologous proteins into the microcompartment. It was estimated that up to 15 000 enzymes may fit into the BMCs, while for Pdu BMCs, where encapsulation is mediated via binding of the enzyme to the shell, a number of 7000 enzymes can be estimated.¹⁶⁵

All three aforementioned BMCs: carboxysomes, Pdu and Eut BMCs allow for the selective targeting of the BMC interior. In β -Carboxysomes, the CcmN C-terminus has been shown to bind to the shell protein CcmK,¹⁷⁵ encouraging the utilization of this interaction to target heterologous enzymes to the carboxysome BMC. Analyzing the function of *Salmonella enterica* genes has identified an N-terminal 19 amino acid sequence at EutC able to localize GFP to the interior of recombinant Eut BMCs.¹⁷⁶ The mechanism for targeted localization of heterologous proteins to

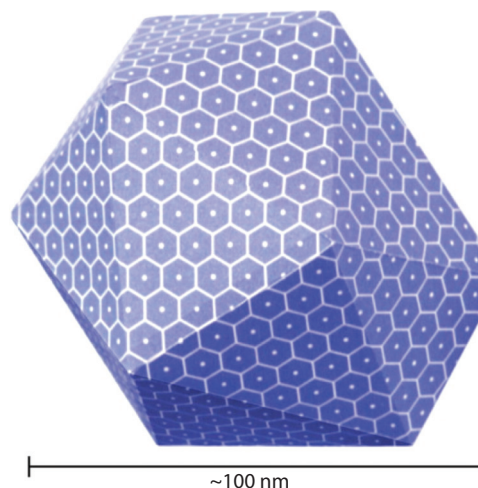


Figure 7. Hypothetical model of the Eut microcompartment emphasizing the construction of a semiregular polyhedron primarily from hexameric shell proteins. Reprinted with the permission from the American Association for the Advancement of Science Copyright® 2010.¹⁷⁴

BMCs has been characterized best for the Pdu BMC system. Three proteins, PduD, PduP and PduV contain a N-terminal sequence sufficient to localize proteins to the lumen of the BMC. The fusion of the N-terminal 18 amino acids of PduD and PduP to target proteins is sufficient to target heterologous proteins to the BMC lumen.^{172,177} In addition, it has been found that the N-terminal 42 amino acids of PduV allow to localize GFP to recombinant Pdu BMCs in *E. coli*, where it is not yet proven if the localization is at the inside or at the outside of the BMC. The regions important for the interaction between PduP and the shell protein PduA,¹⁷⁸ could be revealed by truncation experiments identifying the N-terminal 18 amino acid sequence of PduP and the C-terminal 14 amino acids of PduA to be important for the interaction between the two proteins.

Taken together, BMCs are highly promising candidates to assemble enzyme-based metabolic cascades in various expression systems and biotechnological relevant organism in the future, gaining importance in the context of a sustainable use of natural resources.

8. Protein membrane-based organelles

Protein membrane-based organelles (PMBOs)¹⁷⁹ are a new class of protein-based compartments comprised of amphiphilic proteins self-assembling spontaneously into vesicular organelles *in vivo*. This novel system has been developed recently in the Schiller group introducing a new assembling scheme differing from the assembly of the protein compartments mentioned above. In analogy to amphiphilic lipids, these amphiphilic proteins consist of a hydrophobic and a hydrophilic segment allowing to form dynamic vesicular compartments. In contrast to lipids, proteins have the advantage that they can be synthesized under direct genetic control

allowing to introduce novel bioorthogonal reactivities via UAA²⁷ cotranslationally. First, results show that it is possible to covalently modify these ‘*de novo organelles*’ with small molecules *in vivo*¹⁷⁹ (Figure 1 right: amphiphilic protein-organelles). This approach can be envisioned to be the far reaching start to encode an artificial organelle as nanoreactor *de novo* creating new combinations of natural and artificial catalysts grouping (bio)chemical reactions via the nanoscale assembly of enzymes/catalysts. Strategies like genetically encoded of synthetic organelles are important steps toward controllable ‘production-organism’ in metabolic engineering, synthetic biology and biotechnology.

9. Conclusion and outlook

The development and application of natural and functionalized nanocompartments based on functional proteins is a rapid developing field in nanobiotechnology. Therefore, an overview over the protein-based compartments is thought to facilitate the application and development of innovative protein-based compartments and nanoreactors. Currently, a major focus of protein cage application can be found in the area of biomineralization and nanoparticle templating, but recently, the functional equipment of protein cages with enzymes is gaining momentum. In this review, different types of protein-based nanocompartments and structures have been described. They range from toroid/donut/ring-shaped proteins such as SP1 and Hcp1 allowing to enclose nanoparticles and novel catalytic sites, over nanotubes and cages such as thermosomes used for the polymerization of defined polymers and vault cages able to enclose huge protein complexes, to BMCs naturally equipped with enzymes and PMBOs resembling a lipid membrane substituting amphiphilic lipids with amphiphilic proteins to form a membrane. The selectivity of novel bioconjugation techniques to site-selectively modify proteins by adding novel functionalities *in vivo* will allow to combine the proteinaceous world with the vast possibilities of the chemical tool box in synthetic chemistry. Since all these protein structures and building blocks can be synthesized and assembled *in vivo*, future works aims at the construction of designer organelles which might render new platforms to assemble engineered metabolic cascades in the living cell expanding the functional repertoire to access novel drugs, raw materials and biofuel.

Acknowledgements

The authors thank the Freiburg Institute for Advanced Studies (FRIAS), the Institute for Macromolecular Chemistry, the Centre for Biological Signalling Studies (BOSS), University of Freiburg/Deutsche Forschungsgemeinschaft DFG (german science foundation, EXC 294), the ‘Kompetenznetz funktionelle Nanostrukturen’ (competence network of functional nanostructures, KFN), the Baden-Württemberg Stiftung, the Ministerium für Wissenschaft, Forschung und Kunst (MWK) des Landes Baden-Württemberg (Ministry of Science, Research and Arts Baden-Württemberg) and the Rectorate of the University of Freiburg for support.

REFERENCES

1. Diekmann, Y.; Pereira-Leal, J. B. Evolution of intracellular compartmentalization. *Biochemical Journal* **2013**, *449*(2), 319–331.
2. Fuerst, J. A. Intracellular compartmentation in planctomycetes. *Annual Review of Microbiology* **2005**, *59*(1), 299–328.
3. Bode, S. A.; Minten, I. J.; Nolte, R. J. M.; Cornelissen, J. J. L. M. Reactions inside nanoscale protein cages. *Nanoscale* **2011**, *3*(6), 2376–2389.
4. LeDuc, P. R.; Wong, M. S.; Ferreira, P. M.; Groff, R. E.; Haslinger, K.; Koonce, M. P. Towards an *in vivo* biologically inspired nanofactory. *Nature Nanotechnology* **2007**, *2*(1), 3–7.
5. Renggli, K.; Baumann, P.; Langowska, K.; Onaca, O.; Bruns, N.; Meier, W. Selective and responsive nanoreactors. *Advanced Functional Materials* **2011**, *21*(7), 1241–1259.
6. Kim, K. T.; Meeuwissen, S. A.; Nolte, R. J. M.; van Hest, J. C. M. Smart nanocontainers and nanoreactors. *Nanoscale* **2010**, *2*(6), 844–858.
7. Agapakis, C. M.; Boyle, P. M.; Silver, P. A. Natural strategies for the spatial optimization of metabolism in synthetic biology. *Nature Chemical Biology* **2012**, *8*(6), 527–535.
8. Shuler, M. L.; Foley, P.; Atlas, J. Modeling a minimal cell. *Microbial Systems Biology* **2012**, *881*, 573–610. See http://link.springer.com/protocol/10.1007/978-1-61779-827-6_20 for further details.
9. Luisi, P. L.; Ferri, F.; Stano, P. Approaches to semi-synthetic minimal cells: a review. *Naturwissenschaften* **2006**, *93*(1), 1–13.
10. Peters, R. J. R. W.; Louzao, I.; van Hest, J. C. M. From polymeric nanoreactors to artificial organelles. *Chemical Science* **2012**, *3*(2), 335–342.
11. Ganta, S.; Devalapally, H.; Shahiwal, A.; Amiji, M. A review of stimuli-responsive nanocarriers for drug and gene delivery. *Journal of Controlled Release* **2008**, *126*(3), 187–204.
12. Kundu, P. P.; Sharma, V. Synthetic polymeric vectors in gene therapy. *Current Opinion in Solid State and Materials Science* **2008**, *12*(5–6), 89–102.
13. Comellas-Aragonès, M.; Engelkamp, H.; Claessen, V. I.; Sommerdijk, N. A. J. M.; Rowan, A. E.; Christianen, P. C. M.; Maan, J. C.; Verduin, B. J. M.; Cornelissen, J. J. L. M.; Nolte, R. J. M. A virus-based single-enzyme nanoreactor. *Nature Nanotechnology* **2007**, *2*(10), 635–639.
14. Elzoghby, A. O.; Samy, W. M.; Elgindy, N. A. Protein-based nanocarriers as promising drug and gene delivery systems. *Journal of Controlled Release* **2012**, *161*(1), 38–49.
15. de la Escosura, A.; Nolte, R. J. M.; Cornelissen, J. J. L. M. Viruses and protein cages as nanocontainers and nanoreactors. *Journal of Materials Chemistry* **2009**, *19*(16), 2274–2278.
16. Malinova, V.; Nallani, M.; Meier, W. P.; Sinner, E. K. Synthetic biology, inspired by synthetic chemistry. *FEBS Letters* **2012**, *586*(15), 2146–2156.

17. Vriezema, D. M.; Comellas Aragonès, M.; Elemans, J. A. A. W.; Cornelissen, J. J. L. M.; Rowan, A. E.; Nolte, R. J. M. Self-assembled nanoreactors. *Chemical Reviews* **2005**, *105*(4), 1445–1489.
18. Retterer, S. T.; Simpson, M. L. Microscale and nanoscale compartments for biotechnology. *Current Opinion in Biotechnology* **2012**, *23*(4), 522–528.
19. Dgany, O.; Gonzalez, A.; Sofer, O.; Wang, W.; Zolotnitsky, G.; Wolf, A.; Shoseyov, O.; Almog, O. The structural basis of the thermostability of SP1, a novel plant (*Populus tremula*) boiling stable protein. *Journal of Biological Chemistry* **2004**, *279*(49), 51516–51523.
20. Young, T. S.; Schultz, P. G. Beyond the canonical 20 amino acids: expanding the genetic lexicon. *Journal of Biological Chemistry* **2010**, *285*(15), 11039–11044.
21. Xie, J.; Schultz, P. G. A chemical toolkit for proteins – an expanded genetic code. *Nature Reviews Molecular Cell Biology* **2006**, *7*(10), 775–782.
22. Wang, L.; Schultz, P. G. Expanding the genetic code. *Angewandte Chemie International Edition* **2005**, *44*(1), 34–66.
23. Chin, J. W.; Cropp, T. A.; Anderson, J. C.; Mukherji, M.; Zhang, Z.; Schultz, P. G. An expanded eukaryotic genetic code. *Science* **2003**, *301*(5635), 964–967.
24. Wang, L.; Brock, A.; Herberich, B.; Schultz, P. G. Expanding the genetic code of *Escherichia coli*. *Science* **2001**, *292*(5516), 498–500.
25. Wang, J.; Schiller, S. M.; Schultz, P. G. A biosynthetic route to dehydroalanine-containing proteins. *Angewandte Chemie* **2007**, *119*(36), 6973–6975.
26. Tsao, M.-L.; Tian, F.; Schultz, P. G. Selective staubinger modification of proteins containing p-azidophenylalanine. *ChemBioChem* **2005**, *6*(12), 2147–2149.
27. Chin, J. W.; Santoro, S. W.; Martin, A. B.; King, D. S.; Wang, L.; Schultz, P. G. Addition of p-azido-l-phenylalanine to the genetic code of *Escherichia coli*. *Journal of the American Chemical Society* **2002**, *124*(31), 9026–9027.
28. Deiters, A.; Schultz, P. G. *In vivo* incorporation of an alkyne into proteins in *Escherichia coli*. *Bioorganic & Medicinal Chemistry Letters* **2005**, *15*(5), 1521–1524.
29. Chin, J. W.; Martin, A. B.; King, D. S.; Wang, L.; Schultz, P. G. Addition of a photocrosslinking amino acid to the genetic code of *Escherichia coli*. *Proceedings of the National Academy of Sciences of the United States of America* **2002**, *99*(17), 11020–11024.
30. Dougherty, D. A. Unnatural amino acids as probes of protein structure and function. *Current Opinion in Chemical Biology* **2000**, *4*(6), 645–652.
31. Borrmann, A.; Milles, S.; Plass, T.; Dommerholt, J.; Verkade, J. M. M.; Wiessler, M.; Schultz, C.; van Hest, J. C.; van Delft, F. L.; Lemke, E. A. Genetic encoding of a bicyclo[6.1.0]nonyne-charged amino acid enables fast cellular protein imaging by metal-free ligation. *ChemBioChem* **2012**, *13*(14), 2094–2099.
32. Farrell, I. S.; Toroney, R.; Hazen, J. L.; Mehl, R. A.; Chin, J. W. Photo-cross-linking interacting proteins with a genetically encoded benzophenone. *Nature Methods* **2005**, *2*(5), 377–384.
33. Wang, W.-X.; Pelah, D.; Alergand, T.; Shoseyov, O.; Altman, A. Characterization of SP1, a stress-responsive, boiling-soluble, homo-oligomeric protein from Aspen. *Plant Physiology* **2002**, *130*(2), 865–875.
34. Wang, W.; Dgany, O.; Dym, O.; Altman, A.; Shoseyov, O.; Almog, O. Crystallization and preliminary X-ray crystallographic analysis of SP1, a novel chaperone-like protein. *Acta Crystallographica Section D* **2003**, *59*(3), 512–514.
35. Behrens, S.; Heyman, A.; Maul, R.; Essig, S.; Steigerwald, S.; Quintilla, A.; Wenzel, W.; Bürck, J.; Dgany, O.; Oded Shoseyov, O. Constrained synthesis and organization of catalytically active metal nanoparticles by self-assembled protein templates. *Advanced Materials* **2009**, *21*(34), 3515–3519.
36. Heyman, A.; Medalsy, I.; Bet Or, O.; Dgany, O.; Gottlieb, M.; Porath, D.; Shoseyov, O. Protein scaffold engineering towards tunable surface attachment. *Angewandte Chemie* **2009**, *121*(49), 9454–9458.
37. Medalsy, I.; Dgany, O.; Sowwan, M.; Cohen, H.; Yukashevskaya, A.; Wolf, S. G.; Koster, A.; Almog, O.; Marton, I.; Pouny, Y.; Altman, A.; Shoseyov, O.; Porath, D. SP1 protein-based nanostructures and arrays. *Nano Letters* **2008**, *8*(2), 473–477.
38. Mougous, J. D.; Cuff, M. E.; Raunser, S.; Shen, A.; Zhou, M.; Gifford, C. A.; Goodman, A. L.; Joachimiak, G.; Ordoñez, C. L.; Lory, S.; Walz, T.; Joachimiak, A.; Mekalanos, J. J. A virulence locus of *Pseudomonas aeruginosa* encodes a protein secretion apparatus. *Science* **2006**, *312*(5779), 1526–1530.
39. Zhou, Y.; Tao, J.; Yu, H.; Ni, J.; Zeng, L.; Teng, Q.; Kim, K. S.; Zhao, G. P.; Guo, X.; Yao, Y. Hcp family proteins secreted via the type VI Secretion system coordinately regulate *Escherichia coli* K1 interaction with human brain microvascular endothelial cells. *Infection and Immunity* **2012**, *80*(3), 1243–1251.
40. Cascales, E. The type VI secretion tool kit. *EMBO Reports* **2008**, *9*(8), 735–741.
41. Ballister, E. R.; Lai, A. H.; Zuckermann, R. N.; Cheng, Y.; Mougous, J. D. *In vitro* self-assembly of tailorable nanotubes from a simple protein building block. *Proceedings of the National Academy of Sciences of the United States of America* **2008**, *105*(10), 3733–3738.
42. Schreiber, A.; Zaitseva, E.; Thomann, Y.; Thomann, R.; Dengjel, J.; Hanselmann, R.; Schiller, S. M. Protein yocrowell nanoarchitectures: assembly of donut shaped protein containers and nanofibres. *Soft Matter* **2011**, *7*(6), 2875–2878.

43. Schreiber, A.; Yuan, Y.; Huber, M. C.; Thomann, R.; Ziegler, A.; Cölfen, H.; Dengjel, J.; Krüger, M.; Schiller, S. M. From bioconjugation to self-assembly in nanobiotechnology: Quantum dots trapped and stabilized by toroid protein yocotowsells. *Advanced Engineering Materials* **2012**, *14*(6), B344–B350.
44. Wang, Q.; Lin, T.; Johnson, J. E.; Finn, M. Natural supramolecular building blocks: cysteine-added mutants of cowpea mosaic virus. *Chemistry & Biology* **2002**, *9*(7), 813–819.
45. Wang, W.-X.; Dgany, O.; Wolf, S. G.; Levy, I.; Algom, R.; Pouny, Y.; Wolf, A.; Marton, I.; Altman, A.; Shoseyov, O. Aspen SP1, an exceptional thermal, protease and detergent-resistant self-assembled nano-particle. *Biotechnology and Bioengineering* **2006**, *95*(1), 161–168.
46. Zwickl, P.; Pfeifer, G.; Lottspeich, F.; Kopp, F.; Dahlmann, B.; Baumeister, W. Electron microscopy and image analysis reveal common principles of organization in two large protein complexes: GroEL-type proteins and proteasomes. *Journal of Structural Biology* **1990**, *103*(3), 197–203.
47. Kusmierczyk, A. R.; Martin, J. Chaperonins – keeping a lid on folding proteins. *FEBS Letters* **2001**, *505*(3), 343–347.
48. Braig, K.; Otwinowski, Z.; Hegde, R.; Boisvert, D. C.; Joachimiak, A.; Horwich, A. L.; Sigler, P. B. The crystal structure of the bacterial chaperonin GroEL at 2.8 Å. *Nature* **1994**, *371*, 578–586. DOI:10.1038/371578a0.
49. Sigler, P. B.; Xu, Z.; Rye, H. S.; Burston, S. G.; Fenton, W. A.; Horwich, A. L. Structure and function in GroEL-mediated protein folding. *Annual Review of Biochemistry* **1998**, *67*(1), 581–608.
50. Roseman, A. M.; Chen, S.; White, H.; Braig, K.; Saibil, H. R. The chaperonin ATPase cycle: mechanism of allosteric switching and movements of substrate-binding domains in GroEL. *Cell* **1996**, *87*(2), 241–251.
51. Ranson, N. A.; Farr, G. W.; Roseman, A. M.; Gowen, B.; Fenton, W. A.; Horwich, A. L.; Saibil, H. R. ATP-bound states of GroEL captured by cryo-electron microscopy. *Cell* **2001**, *107*(7), 869–879.
52. Ishii, D.; Kinbara, K.; Ishida, Y.; Ishii, N.; Okochi, M.; Yohda, M.; Aida, T. Chaperonin-mediated stabilization and ATP-triggered release of semiconductor nanoparticles. *Nature* **2003**, *423*(6940), 628–632.
53. Biswas, S.; Kinbara, K.; Oya, N.; Ishii, N.; Taguchi, H.; Aida, T. A tubular biocontainer: metal ion-induced 1d assembly of a molecularly engineered chaperonin. *Journal of the American Chemical Society* **2009**, *131*(22), 7556–7557.
54. Sigg, S. J.; Seidi, F.; Renggli, K.; Silva, T. B.; Kali, G.; Bruns, N. Atom transfer radical polymerization with protein-conjugated catalysts easy removal of copper traces and controlled radical polymerizations in protein nanoreactors. *American Chemical Society* **2011**, *52*, 521–522.
55. Ditzel, L.; Löwe, J.; Stock, D.; Stetter, K.-O.; Huber, H.; Huber, R.; Steinbacher, S. Crystal structure of the thermosome, the archaeal chaperonin and homolog of CCT. *Cell* **1998**, *93*(1), 125–138.
56. Zhang, J.; Baker, M. L.; Schröder, G. F.; Douglas, N. R.; Reissmann, S.; Jakana, J.; Dougherty, M.; Fu, J. C.; Levitt, M.; Ludtke, S. J.; Frydman, J.; Chiu, W. Mechanism of folding chamber closure in a group II chaperonin. *Nature* **2010**, *463*(7279), 379–383.
57. Meyer, A. S.; Gillespie, J. R.; Walther, D.; Millet, I. S.; Doniach, S.; Frydman, J. Closing the folding chamber of the eukaryotic chaperonin requires the transition state of ATP hydrolysis. *Cell* **2003**, *113*(3), 369–381.
58. Reissmann, S.; Parnot, C.; Booth, C. R.; Chiu, W.; Frydman, J. Essential function of the built-in lid in the allosteric regulation of eukaryotic and archaeal chaperonins. *Nature Structural & Molecular Biology* **2007**, *14*(5), 432–440.
59. Bruns, N.; Pustelny, K.; Bergeron, L. M.; Whitehead, T. A.; Clark, D. S. Mechanical nanosensor based on FRET within a thermosome: damage-reporting polymeric materials. *Angewandte Chemie International Edition* **2009**, *48*(31), 5666–5669.
60. Cux, O.; Tanaka, K.; Goldberg, A. L. Structure and functions of the 20S and 26S proteasomes. *Annual Review of Biochemistry* **1996**, *65*, 801–847.
61. Lowe, J.; Stock, D.; Jap, B.; Zwickl, P.; Baumeister, W.; Huber, R. Crystal structure of the 20S proteasome from the archaeon *T. acidophilum* at 3.4 Å resolution. *Science* **1995**, *268*(5210), 533–539.
62. Wenzel, T.; Baumeister, W. Conformational constraints in protein degradation by the 20S proteasome. *Nature Structural & Molecular Biology* **1995**, *2*(3), 199–204.
63. Heinemeyer, W.; Ramos, P. C.; Dohmen, R. J. The ultimate nanoscale mincer: assembly, structure and active sites of the 20S proteasome core. *Cellular and Molecular Life Sciences* **2004**, *61*(13), 1562–1578.
64. Yokozeki, K.; Hara, S. A novel and efficient enzymatic method for the production of peptides from unprotected starting materials. *Journal of Biotechnology* **2005**, *115*(2), 211–220.
65. Kumar, I.; Pratt, R. F. Transpeptidation reactions of a specific substrate catalyzed by the streptomyces R61 DD-peptidase: characterization of a chromogenic substrate and acyl acceptor design. *Biochemistry* **2005**, *44*(30), 9971–9979.
66. Chang, T. K.; Jackson, D. Y.; Burnier, J. P.; Wells, J. A. Subtiligase: a tool for semisynthesis of proteins. *Proceedings of the National Academy of Sciences of the United States of America* **1994**, *91*(26), 12544–12548.
67. Bratovanova, E. K.; Petkov, D. D. Glycine flanked by hydrophobic bulky amino acid residues as minimal sequence for effective subtilisin catalysis. *Biochemical Journal* **1987**, *248*(3), 957–960.
68. Elliott, R. J.; Bennet, A. J.; Braun, C. A.; MacLeod, A. M.; Borgford, T. J. Active-site variants of *Streptomyces griseus* protease B with peptide-ligation activity. *Chemistry & Biology* **2000**, *7*(3), 163–171.

69. Joe, K.; Borgford, T. J.; Bennet, A. J. Generation of a thermostable and denaturant-resistant peptide ligase. *Biochemistry* **2004**, 43(24), 7672–7677.
70. Kim, H. M.; Yu, Y.; Cheng, Y. Structure characterization of the 26S proteasome. *Biochimica et Biophysica Acta* **2011**, 1809(2), 67–79.
71. Deng, Q. Y.; Yang, B.; Wang, J. F.; Whiteley, C. G.; Wang, X. N. Biological synthesis of platinum nanoparticles with apoferritin. *Biotechnology Letters* **2009**, 31(10), 1505–1509.
72. Mukherjee, S.; Sushma, V.; Patra, S.; Barui, A. K.; Bhadra, M. P.; Sreedhar, B.; Patra, C. R. Green chemistry approach for the synthesis and stabilization of biocompatible gold nanoparticles and their potential applications in cancer therapy. *Nanotechnology* **2012**, 23(45), 455103.
73. Gálvez, N.; Valero, E.; Domínguez-Vera, J. M.; Masciocchi, N.; Guagliardi, A.; Clemente-León, M.; Coronado, E. Structural and magnetic characterization of Pd nanoparticles encapsulated in apoferritin. *Nanotechnology* **2010**, 21(27), 274017.
74. Sennuga, A.; Van Marwijk, J.; Whiteley, C. G. Multiple fold increase in activity of ferroxidase–apoferritin complex by silver and gold nanoparticles. *Nanomedicine: Nanotechnology, Biology and Medicine* **2013**, 9(2), 185–193.
75. Sennuga, A.; Van Marwijk, J.; Whiteley, C. G. Ferroxidase activity of apoferritin is increased in the presence of platinum nanoparticles. *Nanotechnology* **2012**, 23(3), 035102.
76. San, B. H.; Kim, S.; Moh, S. H.; Lee, H.; Jung, D.-Y.; Kim, K. K. Platinum nanoparticles encapsulated by aminopeptidase: a multifunctional bioinorganic nanohybrid catalyst. *Angewandte Chemie International Edition* **2011**, 50(50), 11924–11929.
77. Ford, G. C.; Harrison, P. M.; Rice, D. W.; Smith, J. M. A.; Treffry, A.; White, J. L.; Yariv, J. Ferritin: design and formation of an iron-storage molecule. *Philosophical Transactions of the Royal Society B* **1984**, 304(1121), 551–565.
78. Chasteen, N. D.; Harrison, P. M. Mineralization in ferritin: an efficient means of iron storage. *Journal of Structural Biology* **1999**, 126(3), 182–194.
79. Gallois, B.; D'Estaintot, B. L.; Michaux, M.-A.; Dautant, A.; Granier, T.; Précigoux, G.; Soruco, J.-A.; Roland, F.; Chavas-Alba, O.; Herbas, A.; Crichton, R. R. X-ray structure of recombinant horse L-chain apoferritin at 2.0 Å resolution: implications for stability and function. *Journal of Biological Inorganic Chemistry* **1997**, 2(3), 360–367.
80. Sun, S.; Arosio, P.; Levi, S.; Chasteen, N. D. Ferroxidase kinetics of human liver apoferritin, recombinant H-chain apoferritin, and site-directed mutants. *Biochemistry* **1993**, 32(36), 9362–9369.
81. Meldrum, F. C.; Wade, V. J.; Nimmo, D. L.; Heywood, B. R.; Mann, S. Synthesis of inorganic nanophase materials in supramolecular protein cages. *Nature* **1991**, 349(6311), 684–687. DOI:10.1038/349684a0.
82. Meldrum, F. C.; Heywood, B. R.; Mann, S. Magnetoferritin: *in vitro* synthesis of a novel magnetic protein. *Science* **1992**, 257(5069), 522–523.
83. Ueno, T.; Suzuki, M.; Goto, T.; Matsumoto, T.; Nagayama, K.; Watanabe, Y. Size-selective olefin hydrogenation by a pd nanocluster provided in an apo-ferritin cage. *Angewandte Chemie International Edition* **2004**, 43(19), 2527–2530.
84. Zachary, V.; Chad, S.; Peters, J. W.; Mark, Y.; Trevor, D. Biomimetic synthesis of an active H₂ catalyst using the ferritin protein cage architecture. *Biomolecular Catalysis* **2008**, 968, 263–272. See <http://dx.doi.org/10.1021/bk-2008-0986.ch017> for further details.
85. Kang, S.; Lucon, J.; Varpness, Z. B.; Liepold, L.; Uchida, M.; Willits, D.; Young, M.; Douglas, T. Monitoring biomimetic platinum nanocluster formation using mass spectrometry and cluster-dependent H₂ production. *Angewandte Chemie International Edition* **2008**, 47(41), 7845–7848.
86. Varpness, Z.; Peters, J. W.; Young, M.; Douglas, T. Biomimetic synthesis of a H₂ catalyst using a protein cage architecture. *Nano Letter* **2005**, 5(11), 2306–2309.
87. Ilari, A.; Stefanini, S.; Chiancone, E.; Tsernoglou, D. The dodecameric ferritin from *Listeria innocua* contains a novel intersubunit iron-binding site. *Nature Structural & Molecular Biology* **2000**, 7(1), 38–43.
88. Kim, K. K.; Kim, R.; Kim, S.-H. Crystal structure of a small heat-shock protein. *Nature* **1998**, 394(6693), 595–599.
89. Bova, M. P.; Huang, Q.; Ding, L.; Horwitz, J. Subunit exchange, conformational stability, and chaperone-like function of the small heat shock protein 16.5 from *Methanococcus jannaschii*. *Journal of Biological Chemistry* **2002**, 277(41), 38468–38475.
90. Abedin, M. J.; Liepold, L.; Suci, P.; Young, M.; Douglas, T. Synthesis of a cross-linked branched polymer network in the interior of a protein cage. *Journal of the American Chemical Society* **2009**, 131(12), 4346–4354.
91. Flenniken, M. L.; Willits, D. A.; Brumfield, S.; Young, M. J.; Douglas, T. The small heat shock protein cage from *Methanococcus jannaschii* is a versatile nanoscale platform for genetic and chemical modification. *Nano Letters* **2003**, 3(11), 1573–1576.
92. Flenniken, M. L.; Willits, D. A.; Harmsen, A. L.; Liepold, L. O.; Harmsen, A. G.; Young, M. J.; Douglas, T. Melanoma and lymphocyte cell-specific targeting incorporated into a heat shock protein cage architecture. *Chemistry & Biology* **2006**, 13(2), 161–170.
93. Jenni, S.; Leibundgut, M.; Boehringer, D.; Frick, C.; Mikolásek, B.; Ban, N. Structure of fungal fatty acid synthase and implications for iterative substrate shuttling. *Science* **2007**, 316(5822), 254–261.
94. Asturias, F. J.; Chadick, J. Z.; Cheung, I. K.; Stark, H.; Witkowski, A.; Joshi, A. K.; Smith, S. Structure and molecular organization of mammalian fatty acid synthase. *Nature Structural & Molecular Biology* **2005**, 12(3), 225–232.

95. Jenni, S.; Leibundgut, M.; Maier, T.; Ban, N. Architecture of a fungal fatty acid synthase at 5 Å resolution. *Science* **2006**, *311*(5765), 1263–1267.
96. Winton, M. J.; Dubreuil, C. I.; Lasko, D.; Leclerc, N.; McKerracher, L. Characterization of new cell permeable C3-like proteins that inactivate rho and stimulate neurite outgrowth on inhibitory substrates. *Journal of Biological Chemistry* **2002**, *277*(36), 32820–32829.
97. Jung, H.-I.; Cooper, A.; Perham, R. N. Identification of key amino acid residues in the assembly of enzymes into the pyruvate dehydrogenase complex of *Bacillus stearothermophilus*: a kinetic and thermodynamic analysis. *Biochemistry* **2002**, *41*(33), 10446–10453.
98. Dalmau, M.; Lim, S.; Chen, H. C.; Ruiz, C.; Wang, S.-W. Thermostability and molecular encapsulation within an engineered caged protein scaffold. *Biotechnology and Bioengineering* **2008**, *101*(4), 654–664.
99. Domingo, G. J.; Orru, S.; Perham, R. N. Multiple display of peptides and proteins on a macromolecular scaffold derived from a multienzyme complex. *Journal of Molecular Biology* **2001**, *305*(2), 259–267.
100. Schott, K.; Ladenstein, R.; König, A.; Bacher, A. The lumazine synthase-riboflavin synthase complex of *Bacillus subtilis*. Crystallization of reconstituted icosahedral beta-subunit capsids. *Journal of Biological Chemistry* **1990**, *265*(21), 12686–12689.
101. Shenton, W.; Mann, S.; Cölfen, H.; Bacher, A.; Fischer, M. Synthesis of nanophase iron oxide in lumazine synthase capsids. *Angewandte Chemie International Edition* **2001**, *40*(2), 442–445.
102. Seebeck, F. P.; Woycechowsky, K. J.; Zhuang, W.; Rabe, J. P.; Hilvert, D. A simple tagging system for protein encapsulation. *Journal of the American Chemical Society* **2006**, *128*(14), 4516–4517.
103. Kim, D.; San, B. H.; Moh, S. H.; Park, H.; Kim, D. Y.; Lee, S.; Kim, K. K. Structural basis for the substrate specificity of PepA from *Streptococcus pneumoniae*, a dodecameric tetrahedral protease. *Biochemical and Biophysical Research Communications* **2010**, *391*(1), 431–436.
104. Kickhoefer, V. A.; Vasu, S. K.; Rome, L. H. Vaults are the answer, what is the question? *Trends in Cell Biology* **1996**, *6*(5), 174–178.
105. Kong, L. B.; Siva, A. C.; Rome, L. H.; Stewart, P. L. Structure of the vault, a ubiquitous cellular component. *Structure* **1999**, *7*(4), 371–379.
106. Verschoor, A.; Warner, J. R.; Srivastava, S.; Grassucci, R. A.; Frank, J. Three-dimensional structure of the yeast ribosome. *Nucleic Acids Research* **1998**, *26*(2), 655–661.
107. Goldsmith, L. E.; Pupols, M.; Kickhoefer, V. A.; Rome, L. H.; Monbouquette, H. G. Utilization of a protein “shuttle” to load vault nanocapsules with gold probes and proteins. *ACS Nano* **2009**, *3*(10), 3175–3183.
108. Kickhoefer, V. A.; Garcia, Y.; Mikiyas, Y.; Johansson, E.; Zhou, J. C.; Raval-Fernandes, S.; Minoofar, P.; Zink, J. I.; Dunn, B.; Stewart, P. L.; Rome, L. H. Engineering of vault nanocapsules with enzymatic and fluorescent properties. *Proceedings of the National Academy of Sciences of the United States of America* **2005**, *102*(12), 4348–4352.
109. Ludwig, C.; Wagner, R. Virus-like particles – universal molecular toolboxes. *Current Opinion in Biotechnology* **2007**, *18*(6), 537–545.
110. Douglas, T.; Young, M. Viruses: making friends with old foes. *Science* **2006**, *312*(5775), 873–875.
111. Ma, N.; Sargent, E. H.; Kelley, S. O. Biotemplated nanostructures: directed assembly of electronic and optical materials using nanoscale complementarity. *Journal of Materials Chemistry* **2008**, *18*(9), 954.
112. Whyburn, G. P.; Li, Y.; Huang, Y. Protein and protein assembly based material structures. *Journal of Materials Chemistry* **2008**, *18*(32), 3755.
113. Manchester, M.; Singh, P. Virus-based nanoparticles (VNPs): platform technologies for diagnostic imaging. *Advanced Drug Delivery Reviews* **2006**, *58*(14), 1505–1522.
114. Ivanovska, I. L.; de Pablo, P. J.; Ibarra, B.; Sgalari, G.; MacKintosh, F. C.; Carrascosa, J. L.; Schmidt, C. F.; Wuite, G. J. L. Bacteriophage capsids: tough nanoshells with complex elastic properties. *Proceedings of the National Academy of Sciences of the United States of America* **2004**, *101*(20), 7600–7605.
115. Mao, C.; Solis, D. J.; Reiss, B. D.; Kottmann, S. T.; Sweeney, R. Y.; Hayhurst, A.; Georgiou, G.; Iverson, B.; Belcher, A. M. Virus-based toolkit for the directed synthesis of magnetic and semiconducting nanowires. *Science* **2004**, *303*(5655), 213–217.
116. Soto, C. M.; Ratna, B. R. Virus hybrids as nanomaterials for biotechnology. *Current Opinion in Biotechnology* **2010**, *21*(4), 426–438.
117. Speir, J. A.; Munshi, S.; Wang, G.; Baker, T. S.; Johnson, J. E. Structures of the native and swollen forms of cowpea chlorotic mottle virus determined by X-ray crystallography and cryo-electron microscopy. *Structure* **1995**, *3*(1), 63–78.
118. Speir, J. A.; Munshi, S.; Baker, T. S.; Johnson, J. E. Preliminary x-ray data analysis of crystalline cowpea chlorotic mottle virus. *Virology* **1993**, *193*(1), 234–241.
119. Douglas, T.; Strable, E.; Willits, D.; Aitouchen, A.; Libera, M.; Young, M. Protein engineering of a viral cage for constrained nanomaterials synthesis. *Advanced Materials* **2002**, *14*(6), 415–418.
120. Klem, M. T.; Young, M.; Douglas, T. Biomimetic synthesis of α -TiO₂ inside a viral capsid. *Journal of Materials Chemistry* **2008**, *18*(32), 3821.
121. Douglas, T.; Young, M. Host–guest encapsulation of materials by assembled virus protein cages. *Nature* **1998**, *393*(6681), 152–155.

122. de la Escosura, A.; Verwegen, M.; Sikkema, F. D.; Comellas-Aragonès, M.; Kirilyuk, A.; Rasing, T.; Nolte, R. J.; Cornelissen, J. J. Viral capsids as templates for the production of monodisperse Prussian blue nanoparticles. *Chemical Communications* **2008**, 13, 1542–1544.
123. Liepold, L.; Anderson, S.; Willits, D.; Oltrogge, L.; Frank, J. A.; Douglas, T.; Young, M. Viral capsids as MRI contrast agents. *Magnetic Resonance in Medicine* **2007**, 58(5), 871–879.
124. Wu, W.; Hsiao, S. C.; Carrico, Z. M.; Francis, M. B. Genome-free viral capsids as multivalent carriers for taxol delivery. *Angewandte Chemie International Edition* **2009**, 48(50), 9493–9497.
125. Zhao, X.; Fox, J. M.; Olson, N. H.; Baker, T. S.; Young, M. J. *In vitro* assembly of cowpea chlorotic mottle virus from coat protein expressed in *Escherichia coli* and in vitro-transcribed viral cDNA. *Virology* **1995**, 207(2), 486–494.
126. Usselman, R. J.; Walter, E. D.; Willits, D.; Douglas, T.; Young, M.; Singel, D. J. Monitoring structural transitions in icosahedral virus protein cages by site-directed spin labeling. *Journal of the American Chemical Society* **2011**, 133(12), 4156–4159.
127. Minten, I. J.; Hendriks, L. J. A.; Nolte, R. J. M.; Cornelissen, J. J. L. M. Controlled encapsulation of multiple proteins in virus capsids. *Journal of the American Chemical Society* **2009**, 131(49), 17771–17773.
128. Lin, T.; Chen, Z.; Usha, R.; Stauffacher, C. V.; Dai, J.-B.; Schmidt, T.; Johnson, J. E. The refined crystal structure of cowpea mosaic virus at 2.8 Å resolution. *Virology* **1999**, 265(1), 20–34.
129. Wang, Q.; Raja, K. S.; Janda, K. D.; Lin, T.; Finn, M. G. Blue fluorescent antibodies as reporters of steric accessibility in virus conjugates. *Bioconjugate Chemistry* **2003**, 14(1), 38–43.
130. Raja, K. S.; Wang, Q.; Finn, M. G. Icosahedral virus particles as polyvalent carbohydrate display platforms. *ChemBiochem* **2003**, 4(12), 1348–1351.
131. Hooker, J. M.; Kovacs, E. W.; Francis, M. B. Interior surface modification of bacteriophage MS2. *Journal of the American Chemical Society* **2004**, 126(12), 3718–3719.
132. Hooker, J. M.; Datta, A.; Botta, M.; Raymond, K. N.; Francis, M. B. Magnetic resonance contrast agents from viral capsid shells: a comparison of exterior and interior cargo strategies. *Nano Letter* **2007**, 7(8), 2207–2210.
133. Glasgow, J. E.; Capehart, S. L.; Francis, M. B.; Tullman-Ercek, D. Osmolyte-mediated encapsulation of proteins inside MS2 viral capsids. *ACS Nano* **2012**, 6(10), 8658–8664.
134. Fiedler, J. D.; Brown, S. D.; Lau, J. L.; Finn, M. G. RNA-directed packaging of enzymes within virus-like particles. *Angewandte Chemie International Edition* **2010**, 49(50), 9648–9651.
135. Bisht, H.; Weisberg, A. S.; Szajner, P.; Moss, B. Assembly and disassembly of the capsid-like external scaffold of immature virions during vaccinia virus morphogenesis. *Journal of Virology* **2009**, 83(18), 9140–9150.
136. Hyun, J.-K.; Accurso, C.; Hijnen, M.; Schult, P.; Pettikiriachchi, A.; Mitra, A. K.; Coulbaly, F. Membrane remodeling by the double-barrel scaffolding protein of poxvirus. *PLoS Pathogens* **2011**, 7(9), e1002239. See <http://www.ncbi.nlm.nih.gov/pmc/articles/PMC3169552/> for further details.
137. Chen, C.; Daniel, M.-C.; Quinkert, Z. T.; De, M.; Stein, B.; Bowman, V. D.; Chipman, P. R.; Rotello, V. M.; Kao, C. C.; Dragnea, B. Nanoparticle-templated assembly of viral protein cages. *Nano Letter* **2006**, 6(4), 611–615.
138. Patterson, D. P.; Prevelige, P. E.; Douglas, T. Nanoreactors by programmed enzyme encapsulation inside the capsid of the bacteriophage P22. *ACS Nano* **2012**, 6(6), 5000–5009.
139. Patterson, D. P.; Schwarz, B.; El-Boubbou, K.; van der Oost, J.; Prevelige, P. E.; Douglas, T. Virus-like particle nanoreactors: programmed encapsulation of the thermostable CelB glycosidase inside the P22 capsid. *Soft Matter* **2012**, 8(39), 10158–10166.
140. Kanesashi, S.; Ishizu, K.; Kawano, M.; Han, S.; Tomita, S.; Watanabe, H.; Kataoka, K.; Handa, H. Simian virus 40 VP1 capsid protein forms polymorphic assemblies *in vitro*. *Journal of General Virology* **2003**, 84(Pt. 7), 1899–1905.
141. Kawano, M.; Inoue, T.; Tsukamoto, H.; Takaya, T.; Enomoto, T.; Takahashi, R.; Yokoyama, N.; Yamamoto, N.; Nakanishi, A.; Imai, T.; Wada, T.; Kataoka, K.; Handa, H. The VP2/VP3 minor capsid protein of simian virus 40 promotes the *in vitro* assembly of the major capsid protein VP1 into particles. *Journal of Biological Chemistry* **2006**, 281(15), 10164–10173.
142. Kimchi-Sarfaty, C.; Arora, M.; Sandalon, Z.; Oppenheim, A.; Gottesman, M. M. High cloning capacity of *in vitro* packaged SV40 vectors with no SV40 virus sequences. *Human Gene Therapy* **2003**, 14(2), 167–177.
143. Garcea, R. L.; Gissmann, L. Virus-like particles as vaccines and vessels for the delivery of small molecules. *Current Opinion in Biotechnology* **2004**, 15(6), 513–517.
144. Inoue, T.; Kawano, M.; Takahashi, R.; Tsukamoto, H.; Enomoto, T.; Imai, T.; Kataoka, K.; Handa, H. Engineering of SV40-based nano-capsules for delivery of heterologous proteins as fusions with the minor capsid proteins VP2/3. *Journal of Biotechnology* **2008**, 134(1–2), 181–192.
145. Parker, L.; Kendall, A.; Stubbs, G. Surface features of potato virus X from fiber diffraction. *Virology* **2002**, 300(2), 291–295.
146. Lico, C.; Capuano, F.; Renzone, G.; Donini, M.; Marusic, C.; Scaloni, A.; Benvenuto, E.; Baschieri, S. Peptide display on Potato virus X: molecular features of the coat protein-fused peptide affecting cell-to-cell and phloem movement of

- chimeric virus particles. *Journal of General Virology* **2006**, 87(Pt. 10), 3103–3112.
147. Steinmetz, N. F.; Mertens, M. E.; Taurog, R. E.; Johnson, J. E.; Commandeur, U.; Fischer, R.; Manchester, M. Potato virus X as a novel platform for potential biomedical applications. *Nano Letter* **2010**, 10(1), 305–312.
148. Hemminga, M. A.; Vos, W. L.; Nazarov, P. V.; Koehorst, R. B. M.; Wolfs, C. J. A. M.; Spruijt, R. B.; Stopar, D. Viruses: incredible nanomachines. New advances with filamentous phages. *European Biophysics Journal* **2010**, 39(4), 541–550.
149. Carette, N.; Engelkamp, H.; Akpa, E.; Pierre, S. J.; Cameron, N. R.; Christianen, P. C.; Maan, J. C.; Thies, J. C.; Weberskirch, R.; Rowan, A. E.; Nolte, R. J.; Michon, T.; Van Hest, J. C. A virus-based biocatalyst. *Nature Nanotechnology* **2007**, 2(4), 226–229.
150. Nam, K. T.; Kim, D.-W.; Yoo, P. J.; Chiang, C.-Y.; Meethong, N.; Hammond, P. T.; Chiang, Y. T.; Belcher, A. M. Virus-enabled synthesis and assembly of nanowires for lithium ion battery electrodes. *Science* **2006**, 312(5775), 885–888.
151. Yoo, P. J.; Nam, K. T.; Qi, J.; Lee, S.-K.; Park, J.; Belcher, A. M.; Hammond, P. T. Spontaneous assembly of viruses on multilayered polymer surfaces. *Nature Materials* **2006**, 5(3), 234–240.
152. Azucena, C.; Eber, F. J.; Trouillet, V.; Hirtz, M.; Heissler, S.; Franzreb, M.; Fuchs, H.; Wege, C.; Gliemann, H. New approaches for bottom-up assembly of tobacco mosaic virus-derived nucleoprotein tubes on defined patterns on silica- and polymer-based substrates. *Langmuir* **2012**, 28(42), 14867–14877.
153. Knez, M.; Kadri, A.; Wege, C.; Gösele, U.; Jeske, H.; Nielsch, K. Atomic layer deposition on biological macromolecules: metal oxide coating of tobacco mosaic virus and ferritin. *Nano Letter* **2006**, 6(6), 1172–1177.
154. Atanasova, P.; Rothenstein, D.; Schneider, J. J.; Hoffmann, R. C.; Dilfer, S.; Eiben, S.; Wege, C.; Jeske, H.; Bill, J. Virus-templated synthesis of ZnO nanostructures and formation of field-effect transistors. *Advanced Materials Weinheim* **2011**, 23(42), 4918–4922.
155. Balci, S.; Noda, K.; Bittner, A. M.; Kadri, A.; Wege, C.; Jeske, H.; Kern, K. Self-assembly of metal-virus nanodumbbells. *Angewandte Chemie International Edition* **2007**, 46(17), 3149–3151.
156. Balci, S.; Hahn, K.; Kopold, P.; Kadri, A.; Wege, C.; Kern, K.; Bittner, A. M. Electroless synthesis of 3 nm wide alloy nanowires inside tobacco mosaic virus. *Nanotechnology* **2012**, 23(4), 045603.
157. Shively, J. M.; Decker, G. L.; Greenawalt, J. W. Comparative ultrastructure of the *Thiobacilli*. *Journal of Bacteriology* **1970**, 101(2), 618–627.
158. Shively, J. M.; Ball, F.; Brown, D. H.; Saunders, R. E. Functional organelles in prokaryotes: polyhedral inclusions (carboxysomes) of *Thiobacillus neapolitanus*. *Science* **1973**, 182(4112), 584–586.
159. Sutter, M.; Boehringer, D.; Gutmann, S.; Günther, S.; Prangishvili, D.; Loessner, M. J.; Stetter, K. O.; Weber-Ban, E.; Ban, N. Structural basis of enzyme encapsulation into a bacterial nanocompartment. *Nature Structural & Molecular Biology* **2008**, 15(9), 939–947.
160. Corchero, J. L.; Cedano, J. Self-assembling, protein-based intracellular bacterial organelles: emerging vehicles for encapsulating, targeting and delivering therapeutical cargoes. *Microbial Cell Factories* **2011**, 10(1), 92.
161. Yeates, T. O.; Kerfeld, C. A.; Heinhorst, S.; Cannon, G. C.; Shively, J. M. Protein-based organelles in bacteria: carboxysomes and related microcompartments. *Nature Reviews Microbiology* **2008**, 6(9), 681–691.
162. Kerfeld, C. A.; Heinhorst, S.; Cannon, G. C. Bacterial microcompartments. *Annual Review of Microbiology* **2010**, 64(1), 391–408.
163. Cheng, S.; Liu, Y.; Crowley, C. S.; Yeates, T. O.; Bobik, T. A. Bacterial microcompartments: their properties and paradoxes. *Bioessays* **2008**, 30(11–12), 1084–1095.
164. Yeates, T. O.; Crowley, C. S.; Tanaka, S. Bacterial microcompartment organelles: protein shell structure and evolution. *Annual Review of Biophysics* **2010**, 39, 185–205.
165. Kim, E. Y.; Tullman-Ercek, D. Engineering nanoscale protein compartments for synthetic organelles. *Current Opinion in Biotechnology*. See <http://www.sciencedirect.com/science/article/pii/S0958166912002078> for further details.
166. Crowley, C. S.; Cascio, D.; Sawaya, M. R.; Kopstein, J. S.; Bobik, T. A.; Yeates, T. O. Structural insight into the mechanisms of transport across the *Salmonella enterica* Pdu microcompartment shell. *Journal of Biological Chemistry* **2010**, 285(48), 37838–37846.
167. Tsai, Y.; Sawaya, M. R.; Cannon, G. C.; Cai, F.; Williams, E. B.; Heinhorst, S.; Kerfeld, C. A.; Yeates, T. O. Structural analysis of CsoS1A and the protein shell of the *Halothiobacillus neapolitanus* carboxysome. *PLoS Biology* **2007**, 5(6), e144.
168. Kinney, J. N.; Axen, S. D.; Kerfeld, C. A. Comparative analysis of carboxysome shell proteins. *Photosynthesis Research* **2011**, 109(1–3), 21–32.
169. Bonacci, W.; Teng, P. K.; Afonso, B.; Niederholtmeyer, H.; Grob, P.; Silver, P. A.; Savage, D. F. Modularity of a carbon-fixing protein organelle. *Proceedings of the National Academy of Sciences of the United States of America* **2012**, 109(2), 478–483.
170. Espie, G. S.; Kimber, M. S. Carboxysomes: cyanobacterial Rubis CO comes in small packages. *Photosynthesis Research* **2011**, 109(1–3), 7–20.
171. Penrod, J. T.; Roth, J. R. Conserving a volatile metabolite: a role for carboxysome-like organelles in *Salmonella enterica*. *Journal of Bacteriology* **2006**, 188(8), 2865–2874.

-
172. Fan, C.; Cheng, S.; Liu, Y.; Escobar, C. M.; Crowley, C. S.; Jefferson, R. E.; Yeates, T. O.; Bobik, T. A. Short N-terminal sequences package proteins into bacterial microcompartments. *Proceedings of the National Academy of Sciences of the United States of America* **2010**. See <http://www.pnas.org/content/early/2010/03/17/0913199107> for further details.
173. Yeates, T. O.; Thompson, M. C.; Bobik, T. A. The protein shells of bacterial microcompartment organelles. *Current Opinion in Biotechnology* **2011**, *21*(2), 223–231.
174. Tanaka, S.; Sawaya, M. R.; Yeates, T. O. Structure and mechanisms of a protein-based organelle in *Escherichia coli*. *Science* **2010**, *327*(5961), 81–84.
175. Kinney, J. N.; Salmeen, A.; Cai, F.; Kerfeld, C. A. Elucidating essential role of conserved carboxysomal protein CcmN reveals common feature of bacterial microcompartment assembly. *Journal of Biological Chemistry* **2012**, *287*(21), 17729–17736.
176. Choudhary, S.; Quin, M. B.; Sanders, M. A.; Johnson, E. T.; Schmidt-Dannert, C. Engineered protein nano-compartments for targeted enzyme localization. *PLoS One* **2012**, *7*(3), e33342.
177. Fan, C.; Bobik, T. A. The N-terminal region of the medium subunit (PduD) packages adenosylcobalamin-dependent diol dehydratase (PduCDE) into the Pdu microcompartment. *Journal of Bacteriology* **2011**, *193*(20), 5623–5628.
178. Fan, C.; Cheng, S.; Sinha, S.; Bobik, T. A. Interactions between the termini of lumen enzymes and shell proteins mediate enzyme encapsulation into bacterial microcompartments. *Proceedings of the National Academy of Sciences of the United States of America* **2012**, *109*(37), 14995–5000.
179. Huber, M. C.; Schreiber, A.; Varga, B. R.; Kele, P.; Von Olshausen, P.; Schiller, S. M. Programmed nano-engineering of genetically encoded protein tectons: strategy towards higher order architectures forming compartments inside the cell (manuscript submitted).
180. Baumann, R. W. *Microbiology with Diseases by Taxonomy*, 2nd edn. Upper Saddle River: Pearson Education, 2007.
181. Bohm, J.; Frangakis, A. S.; Hegerl, R.; Nickell, S.; Typke, D.; Baumeister, W. Toward detecting and identifying macromolecules in a cellular context: template matching applied to electron tomograms. *Proceedings of the National Academy of Sciences of the United States of America* **2000**, *97*(26), 14245–14250.

WHAT DO YOU THINK?

To discuss this paper, please email up to 500 words to the managing editor at bbn@icepublishing.com

Your contribution will be forwarded to the author(s) for a reply and, if considered appropriate by the editor-in-chief, will be published as a discussion in a future issue of the journal.

ICE Science journals rely entirely on contributions sent in by professionals, academics and students coming from the field of materials science and engineering. Articles should be within 5000–7000 words long (short communications and opinion articles should be within 2000 words long), with adequate illustrations and references. To access our author guidelines and how to submit your paper, please refer to the journal website at www.icevirtuallibrary.com/bbn